Chapter 4

Synthesis, Characterization and Catalytic Application of Abnormal N-heterocyclic Carbene/CNN Pincer Palladium(II) Complex for the Suzuki-Miyaura Reaction in Water

4.1 Introduction

Transition metal-based catalysis is fundamental for the formation of carbon-carbon and carbon-heteroatom bonds to build simple as well as complex molecules [1-4]. Generally, in the presence of a metal catalyst, an electrophilic reagent (mostly organic halides) couples with a nucleophilic reagent (an organometallic reagent, an amine, alkene, alkyne, etc.), which may be either commercially available or readily synthesized. This methodology provides a variety of classical cross-coupling reactions such as Suzuki-Miyaura, Negishi, Stille, Kumada, Hiyama, Buchwald-Hartwig, Heck, Sonogashira, and others. Their development and widespread applications became boisterous after the full recognition of their synthetic utility. The chemistry Nobel Prize 2010 was awarded to Akira Suzuki, Richard F. Heck, and Ei-ichi Negishi for C-C bond formation [5-8]. The Suzuki-Miyaura cross-coupling is a well-known C-C bond-forming reaction due to the involvement of mild reaction conditions. Several metal centres are in principle capable of catalyzing the various steps of the reaction, but undoubtedly palladium-based catalysts dominate the scene due to their unique reactivity [9-10]. Palladium has readily accessible two stable oxidation states, 0 and +2, and reversible interconversion between these two oxidation states is facile. The availability of Pd-containing species with simultaneously one or more empty and filled non-bonding orbitals are some of the important features of palladium complexes as catalysts [11]. Palladium-catalyzed C-C coupling reactions without using any ligands have been reported, but the major drawbacks associated with them is the use of toxic solvents, requirement of high temperature and long reaction time. The palladium-based catalysts are recognized as an indispensable tool for the synthesis of conjugated dienes and higher polyene systems with high stereoisomeric purity. These biaryls (symmetrical, unsymmetrical, and hetero-) have great importance in pharmaceuticals and chemical industry [12-17].

The Suzuki-Miyaura reaction involves palladium-mediated coupling of organic electrophiles with organoboron compounds in the presence of a base. The general catalytic cycle for the Suzuki-Miyaura reaction begins with more stable Pd(II) species which are then reduced to Pd(0) species under *in situ* condition and enter into the catalytic cycle. The initial step of the catalytic cycle is the activation of the aryl halide by oxidative addition to palladium to form the organopalladium species. Further, the organopalladium complex breaks and the transmetalation takes place and the boron-ate complex (produced by the reaction of the boronic acid with base) is formed.

Later the reductive elimination produces the cross-coupled product with the completion of the catalytic process (**Scheme 4.1**) [18-19].

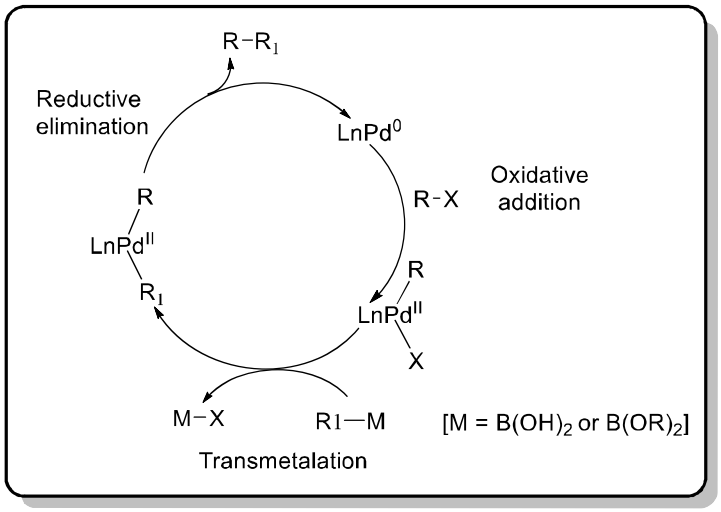

Scheme 4.1 General catalytic cycle for the Suzuki-Miyaura cross-coupling reaction

It is well-known, that in transition metal-based catalysis the activity and selectivity of a catalytic system are influenced by the ligand attached to the metal. Thus, selecting a suitable ligand is an important step to improve catalyst activity. Some literature precedents have described ligand-free Suzuki-Miyaura reaction using simple Pd salts, but they act as precursors for Pd nanoparticles which are actual catalytic species [20-24]. In comparison with ligand-free protocols, ligand based-systems always offer better selectivity and functional group tolerance [25-29]. Previously, the phosphine-based ligands were the preferred class of ligands for the Suzuki-Miyaura reaction due to their tunable steric and electronic properties controlled by the functional groups attached to the phosphorus atom [30-32]. Despite their appealing success, phosphines are not a very desirable class of ligands for catalysis due to their high cost, detrimental environmental features, complicated syntheses, air and moisture instability, and difficulty in handling [33].

Thus, several new phosphine-free catalytic systems mainly based on nitrogen-containing ligands for the Suzuki-Miyaura reaction have been developed. These nitrogen-based systems have many advantages including their easy handling and moisture insensitivity. Thus, a library of N-based ligands, such as amines [34], oxime [35], hydrazone [36], Schiff bases [37] and N-heterocyclic carbenes (NHCs) [38] have been utilized effectively in the Suzuki-Miyaura reactions. Among these ligands, the imidazolium-based NHCs have received special attention,

mainly because of their simple synthesis and higher stability. Moreover, the most attractive characteristic of NHC similar to phosphines is that their steric and electronic properties can be tuned easily, and they can stabilize metal centres in the key catalytic steps. Due to these unique features, NHCs provide highly reactive palladium-based Suzuki-Miyaura coupling catalysts. Their strong σ donor property enables the oxidative addition of unreactive aryl halides and by tuning substituents at the nitrogen atoms enhances the reductive elimination of the product [39-40].

Imidazolium-based NHC ligands usually bind to a metal centre through C2 carbon atom **(1)** termed as normal NHCs (nNHCs), as shown in **Figure 4.1**. But Crabtree *et al*. identified an alternative binding mode *via* C4/C5 atom (**2**/**3**), referred to as abnormal NHCs (aNHCs) [41].

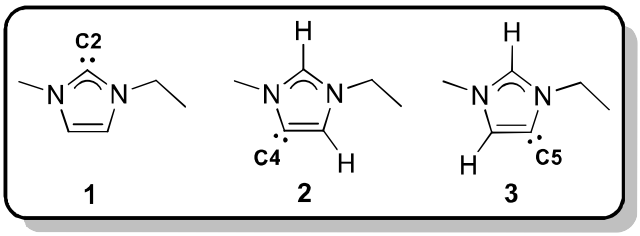

Figure 4.1 Normal (**1**) and abnormal (**2** and **3**) NHCs

Due to the electron richness, aNHCs are considered to be excellent building blocks in designing numerous organometallic catalysts that possess good catalytic activities for various organic reactions [42]. In aNHC, the carbenic centre is near to only one electronegative nitrogen atom while in nNHC two nearby nitrogen atoms are present. aNHC due to its strong σ donation capability binds strongly with a metal centre and presents superior catalytic activity in comparison to its normal NHC counterpart [43-44]. Yang *et al.* reported the synthesis of picolyl functionalized NHC-Pd(II) complexes **4a** and **4b** (**Figure 4.2**) *via* direct metallation of 4,5-diphenyl substituted picolyl hydroxyl di-functionalised imidazolium salts with $PdCl_2$. The complex **4a** and **4b** catalyzed the Suzuki-Miyaura reaction in water efficiently and provided a wide range of functional groups tolerance. Both electron-donating or electron-withdrawing substituted phenylboronic acids and aryl bromides gave moderate to high yields of cross-coupled products [45]. Chen *et al.* synthesized NHC-Pd(II) complexes **5a** and **5b** bearing an N-donor group (**Figure 4.2**) without orthometallation and used them as catalysts in the Suzuki-Miyaura reaction. Sterically hindered inactivated aryl chlorides coupled efficiently with sterically hindered boronic acids and provided di- and tri-*ortho*-substituted biaryls in high yields at room temperature in ethanol under aerobic condition. They suggested that by

removing the orthometallation motif, the complexes shorten the pre-activation step time and showed remarkable catalytic activities [46].

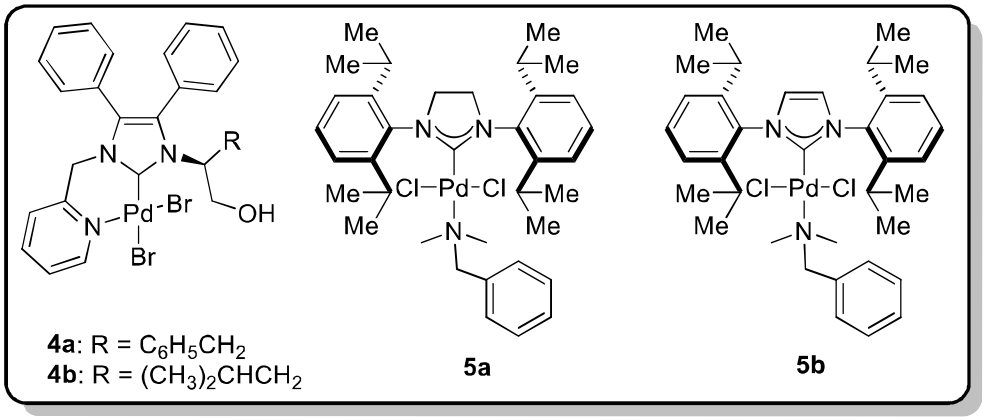

Figure 4.2 Imidazolium-based picolyl functionalised (**4a-b)** and without orthometallation generated (**5a-b)** NHC-Pd(II) catalysts

Steeples *et al.* synthesized five amino acid derived bis- and PEPPSI-type NHC-Pd(II) complexes **6a-e** (**Figure 4.3**) for the aqueous phase Suzuki-Miyaura reaction. Complex **6d** exhibited the best activity among all complexes and **6a** and **6b** were observed to produce moderate conversion. Pinacol ester provided good yields of the products in comparison to boronic acid. It was concluded that the catalysis proceeds through a "catalyst cocktail" model, with Pd-nanoparticles responsible for most of the catalytic activity as evidenced by transmission electron microscopy and mercury poisoning test [47].

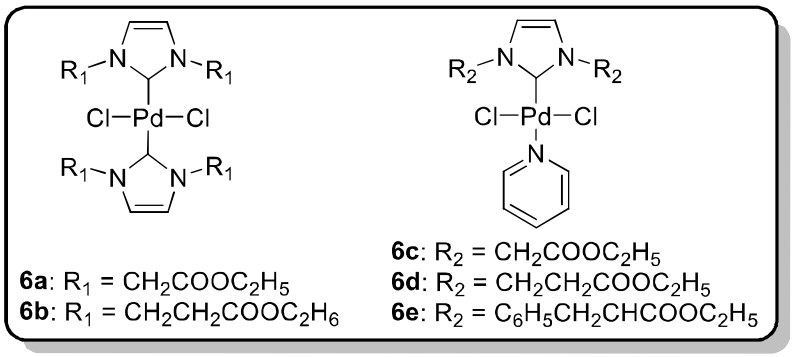

Figure 4.3 Bis- and PEPPSI-type NHC-Pd(II) catalysts (**6a-e**)

Wang *et al.* prepared a series of NHC-Pd(II) complexes **7a-d** (**Figure 4.4**) from commercially available $PdCl_2$, imidazolium salts, and benzoxazole or benzothiazole in one step. The obtained complexes showed efficient catalytic activity for the Suzuki-Miyaura reaction of aryl as well as benzyl chlorides with arylboronic acids in moderate to high yields. Aryl chlorides

with both electron-donating and electron-withdrawing substituents were tolerated and good results were obtained. However, electron-deficient and sterically hindered boronic acids resulted in low product yields. The reaction of benzyl chlorides and substituted arylboronic acids also afforded diarylmethanes in excellent yields [48]. Seva *et al*. reported the synthesis of biphenyl bis-NHC-Pd(II) complexes **8a-c** (**Figure 4.4**) and investigated their catalytic efficiency in the Suzuki-Miyaura reaction in water. The order of reactivity of the complexes was found to be **8a** > **8b** ≫ **8c**. In the case of **8c**, the different electron-donating and withdrawing substituents on phenylboronic acid did not affect the product yield. By using complex **8a**, iodobenzene and bromobenzene provided higher yields of the product while chlorobenzene resulted in poor yields [49].

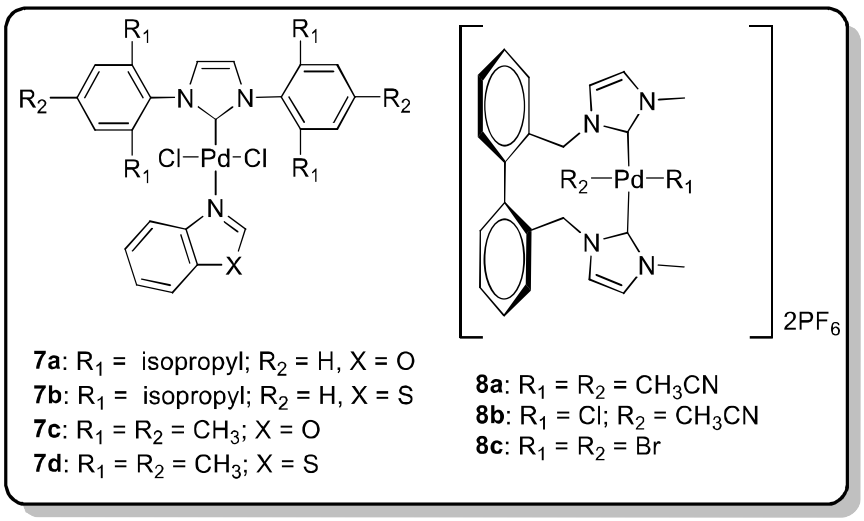

Figure 4.4 Benzoxazole- or benzothiazole- (**7a-d**) and Biphenyl-based (**8a-c**) NHC-Pd(II) catalysts

Garrido *et al*. proposed the synthesis of water-soluble sulfonated NHC-Pd(II) complexes **9a-d** (**Figure 4.5**) and used them as a catalyst in the Suzuki-Miyaura reaction. The complex **9a** was the most active catalyst, due to weaker coordination and stronger solvation of the chloride ligand in protic solvents. It catalyzed the coupling of inactivated and sterically hindered substrates under mild conditions except in the case of most hindered aryl chlorides due to the competitive hydrodehalogenation process [50]. Mandal and coworkers reported the synthesis of halobridged C-H activated aNHC palladium complexes **10a** and **10b** (**Figure 4.5**) and tested their efficiency in the Suzuki-Miyaura cross-coupling of aryl chlorides. The preliminary results indicated that using these complexes aryl chlorides can be activated at room temperature to provide a quantitative yield of the corresponding biphenyls on reaction with

boronic acids. These catalysts exhibited their activity at very low catalyst loading up to 0.005 mol%. DFT studies suggested that the Pd-carbene bond was very strong and prevented the palladium leaching in solution and the catalyst remained active for 10 successive catalytic cycles without much loss in its activity [51].

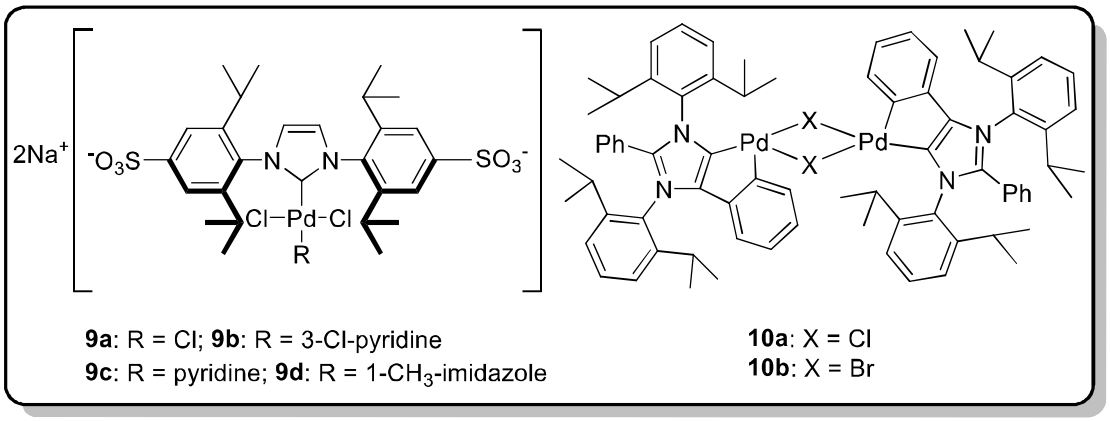

Figure 4.5 Sulfonated (**9a-d**) and Halobridged C-H activated (**10a-b**) aNHC-Pd(II) catalysts

Rottschäfer *et al*. synthesized a series of aNHC complexes **11a-h** (**Figure 4.6**) and investigated the catalytic activity of complexes **11a**, **11c**, and **11d** for the Suzuki-Miyaura coupling reaction at room temperature. The dimeric Pd complex **11a** was found to be more active than **11c** and **11d** [52].

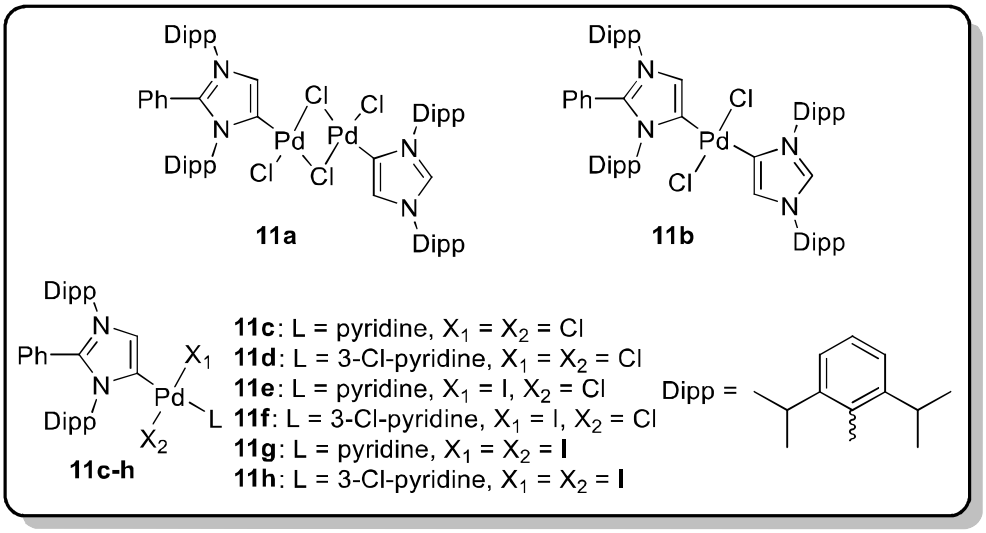

Figure 4.6 C2-arylated imidazolium-based aNHC-Pd(II) catalyst (**11a-h**)

In conjunction with the meteoric rise in the use of NHC ligands, mertridentate "pincer" ligand architectures pervade existing catalysis, providing high thermal stability and supporting a

broad range of metal-based catalysts [53]. Pincer ligands have been used to stabilize complexes *via* chelate effects and the donor atoms. Substituents on the pincer ligands can be varied to control the electron densities on the metal ions [54]. Combining the properties of NHC donors with mertridentate ligand architectures represent a potentially fascinating concept of modern ligand design [55]. Pincer based NHC palladium complexes also have attracted attention for the Suzuki-Miyaura reaction. Wei *et al.* synthesized monoanionic pincer-NHC Pd(II) complexes **12a-c** (**Figure 4.7**) were thermally stable under moisture, air, and at high temperature. They investigated their application for the Suzuki-Miyaura reaction, complex **12a** was found to be more efficient than **12b** and **12c**. They were effective even for the coupling of less activated aryl bromides with phenylboronic acid. A variety of aryl bromides containing both electron-donating and electron-withdrawing substituents were well tolerated with no palladium black formation in reaction [56]. Inés *et al.* reported the synthesis and catalytic application of the pincer-NHC Pd(II) complexes **13a** and **13b** (**Figure 4.7**) for the Suzuki-Miyaura *via* coupling of arylboronic acids with aryl and benzyl bromides in aqueous medium. Good to excellent yields of bi-arylated products were obtained in all cases irrespective of the electronic or steric nature of the coupling partners. Catalyst recycling experiments revealed that increasing the time in every run allowed the recycling of both catalysts up to 13 runs. On keeping the reaction time constant, the effective reuse of the catalyst was reduced to 3 and 7 runs for **13a** and **13b**, respectively [57].

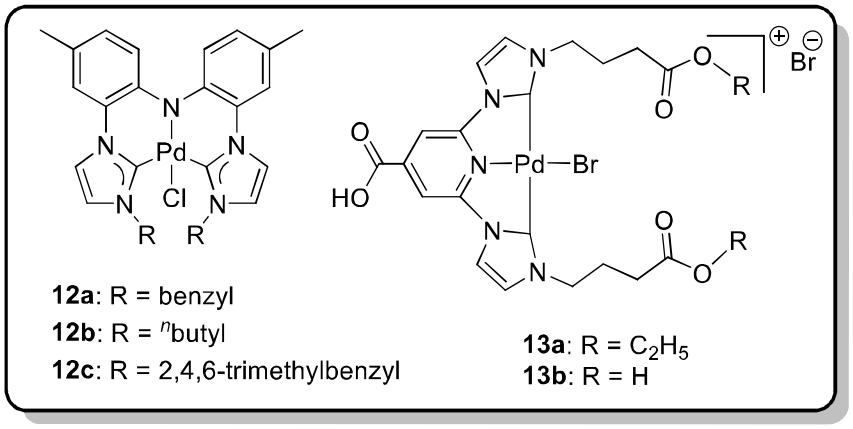

Figure 4.7 CNC pincer type NHC Pd(II) catalyst (**12a-c**) and (**13a-b**)

Imanaka *et al.* synthesized pincer-NHC Pd(II) complexes **14a** and **14b** (**Figure 4.8**) with acetyl-protected D-glucopyranosyl groups in CCN and CNC arrangements. The complexes catalyzed the Suzuki-Miyaura cross-coupling reactions in water with turnover numbers of

75,000 and 8,900 for **14a** and **14b** complexes, respectively. Complex **14a** was not deactivated by the addition of metallic Hg which suggested that the active species was the complex itself. Complex **14b** exhibited no catalytic activity in the presence of metallic Hg, proposing the involvement of heterogeneous catalysts, such as Pd nanoparticles [58]. Haque *et al.* proposed a series of pincer-NHC Pd(II) complexes **15a-e** (**Figure 4.8**) and investigated their catalytic potential for the Suzuki-Miyaura and Heck-Mizoroki reactions of phenylboronic acid and *n*-butyl acrylate with a broad range of activated and deactivated bromobenzene derivatives in aqueous medium. The Suzuki-Miyaura reaction afforded biphenyls in higher yields as compared to the Heck-Mizoroki reaction (except **15b**) [59].

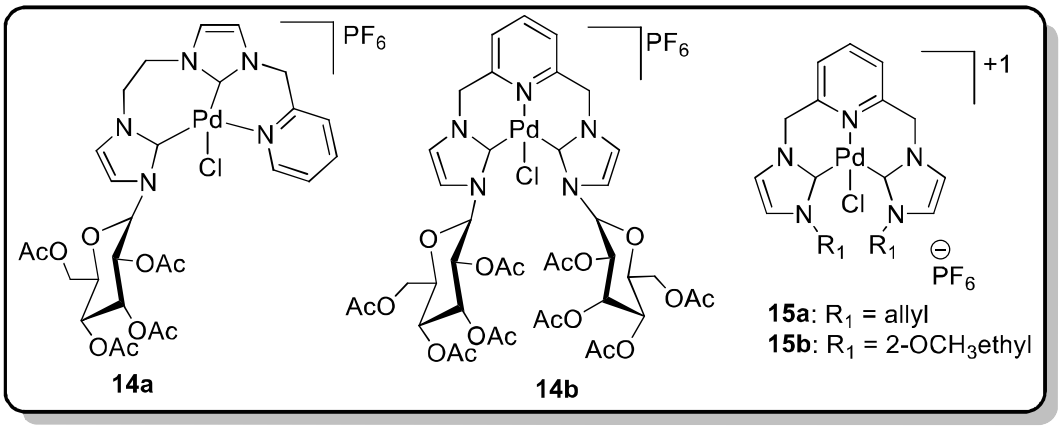

Figure 4.8 Acetyl-protected D-glucopyranosyl-based CCN/CNC (**14a-b**) and Bis-imidazolium derived CNC (**15a-b)** pincer NHC Pd(II) catalysts

It is noteworthy that aryl iodides and bromides are highly expensive substrates in the reaction, whereas chlorides are readily available and cheaper. A considerable research effort has been centred on the synthesis and use of catalysts capable of activating aryl chloride substrates at very low catalyst loading. Therefore, there is a growing demand for developing highly efficient palladium-based catalysts with the aim to work at low catalyst loading, avoid the use of noxious additives, use of less activated aryl chlorides and using water as a solvent. In contribution to ongoing research to achieve an efficient catalytic system an abnormal NHC based palladium(II) complex bearing CNN-pincer architecture is used as a catalyst for the Suzuki-Miyaura cross-coupling reaction. Reaction under microwave irradiation, using water as a solvent and employing less activated aryl chlorides as an aryl halide source are the key features of the present strategy.

4.2 Results and discussion

4.2.1 Synthesis and characterization of L2H and L2PdBr

The synthetic route involved in the preparation of CNN pincer derived NHC ligand **L2H** and its palladium complex **L2PdBr** is summarized in **Scheme 4.2**. N-alkylation of 8-aminoquinoline was done in dioxane using bromoacetic acid to afford 2-bromo-N-(quinolin-8-yl)acetamide and further its quaternization with 1-methylimidazole through simple nucleophilic substitution reaction provided imidazolium-based ligand **L2H**. Its palladium complex **L2PdBr** was obtained by adding palladium acetate to **L2H** in methanol at 70 °C.

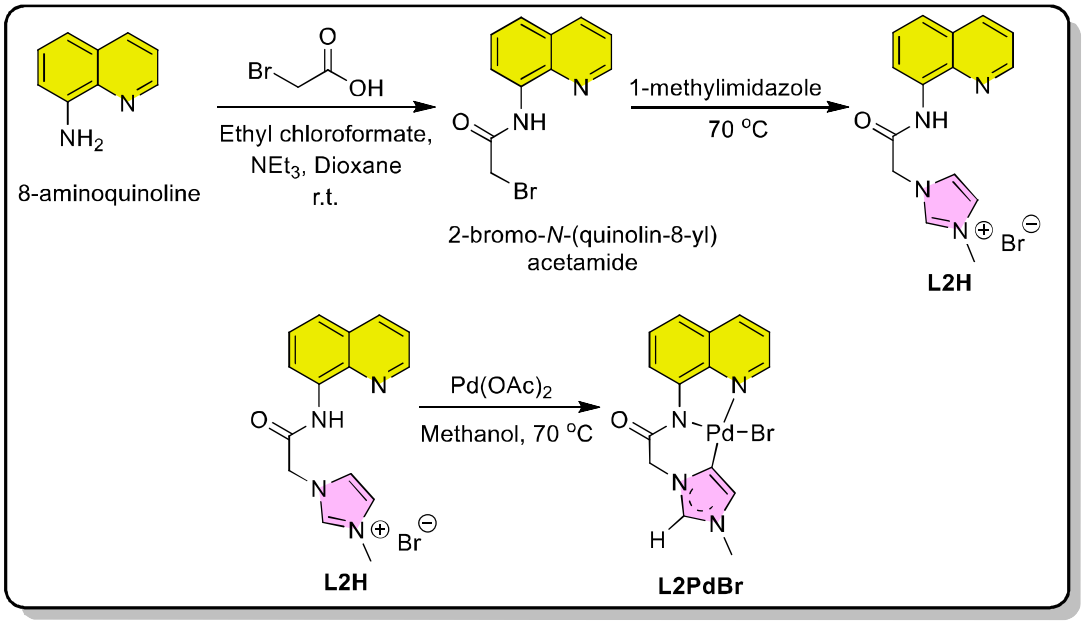

Scheme 4.2 Synthesis of **L2PdBr**

In ^{1}H NMR of **L2H**, the singlet for amidic NH proton (H16) appeared at 10.89 ppm. The signals at 9.00 and 9.23 ppm were assigned to H1 and H12 protons, respectively. The rest two imidazolium and the aromatic proton of the quinoline ring appeared in region 7.59-8.58 ppm. The singlets of aliphatic CH_2 and CH_3 protons were observed at 5.52 and 3.95 ppm, respectively (**Figure 4.9**). The unusual coordination mode of NHC ligand to palladium was proposed on the basis of ^{1}H, ^{13}C, DEPT-135, COSY, HSQC, and HMBC NMR studies and X-ray crystal structure analysis. The 15 proton signals observed in the ^{1}H NMR spectrum of **L2H** reduced to 13 in **L2PdBr**. After coordination, signals observed at 7.83 ppm (H14) and 10.89 ppm (H16) in **L2H** disappeared (**Figure 4.10**). Also, in the ^{13}C NMR spectrum of **L2H**, an

amidic C=O (C10) signal observed at δ 165.1 ppm (**Figure 4.11**) shifted downfield to 167.4 ppm in **L2PdBr** (**Figure 4.12**).

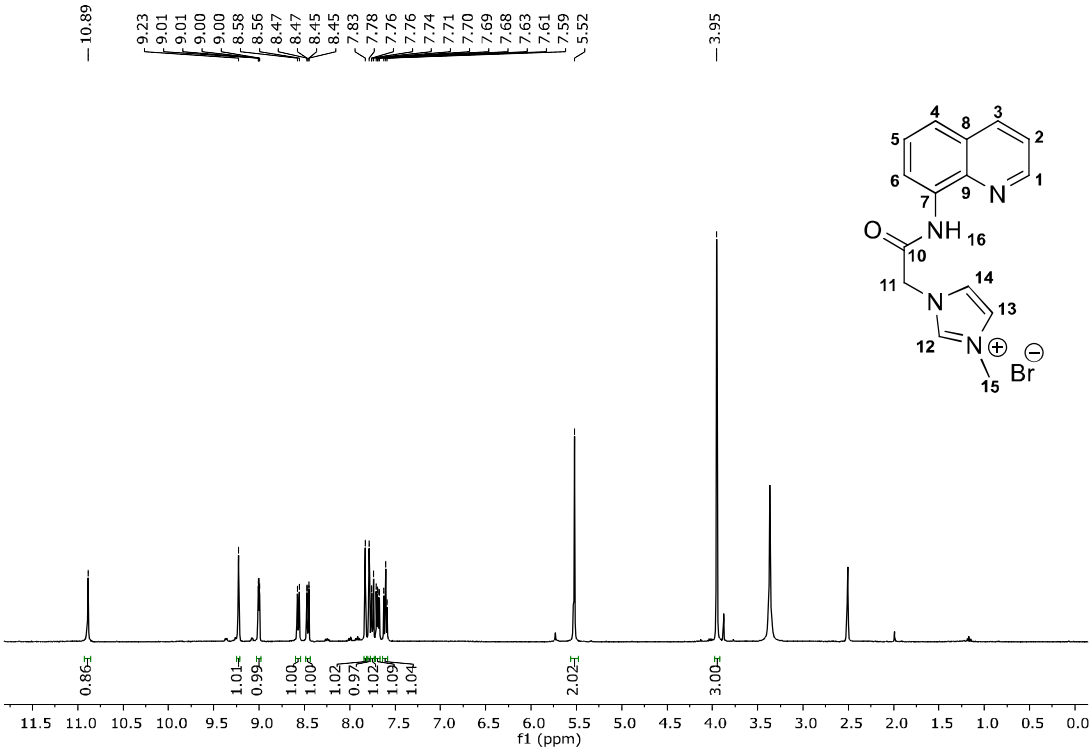

Figure 4.9 ^{1}H NMR spectrum of **L2H** (DMSO-d_6)

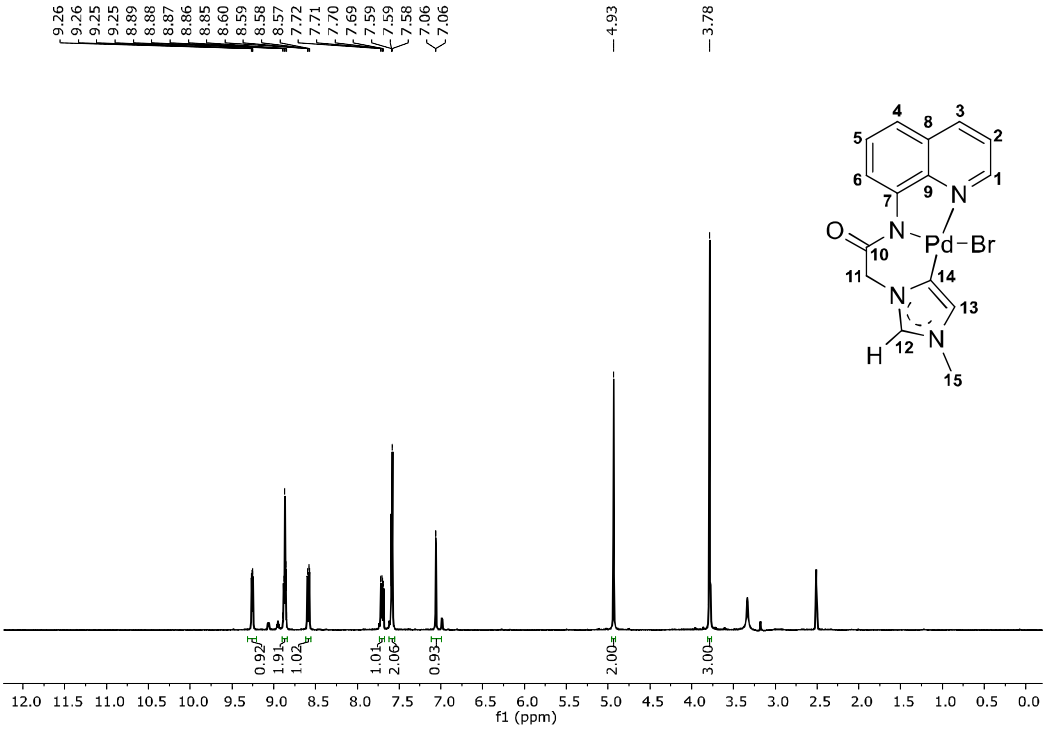

Figure 4.10 ^{1}H NMR spectrum of **L2PdBr** (DMSO-d_6)

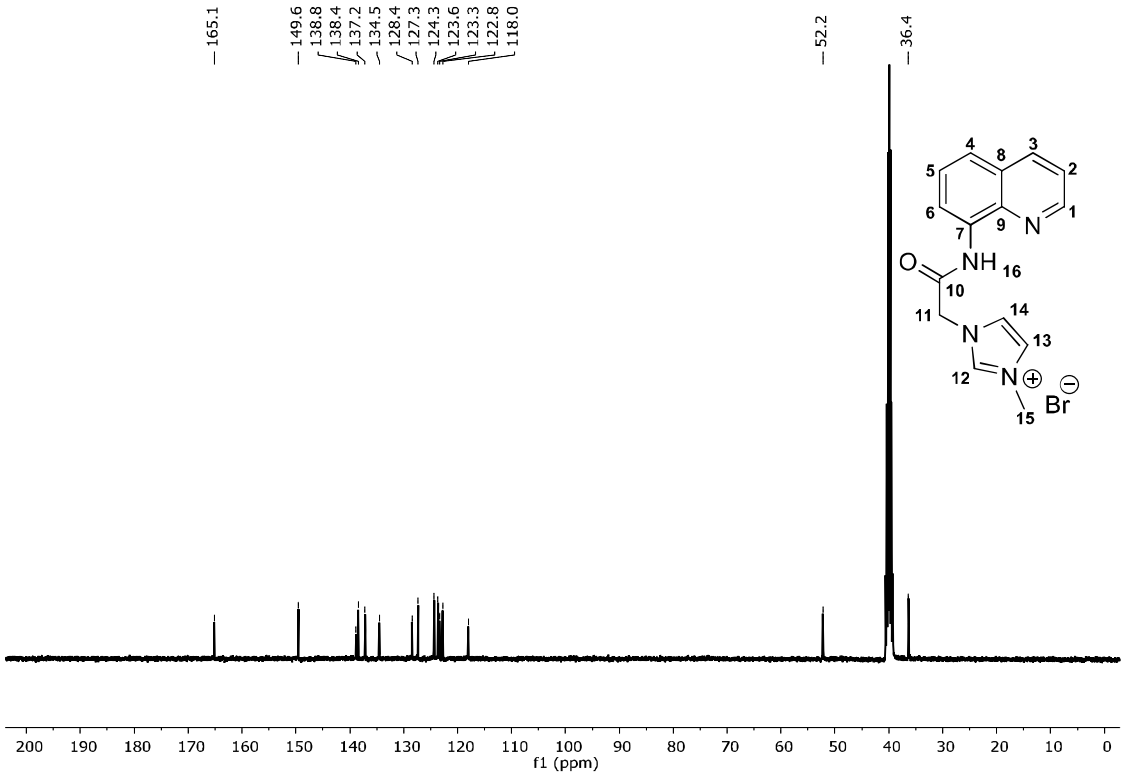

Figure 4.11 ^{13}C NMR spectrum of **L2H** (DMSO-d_6)

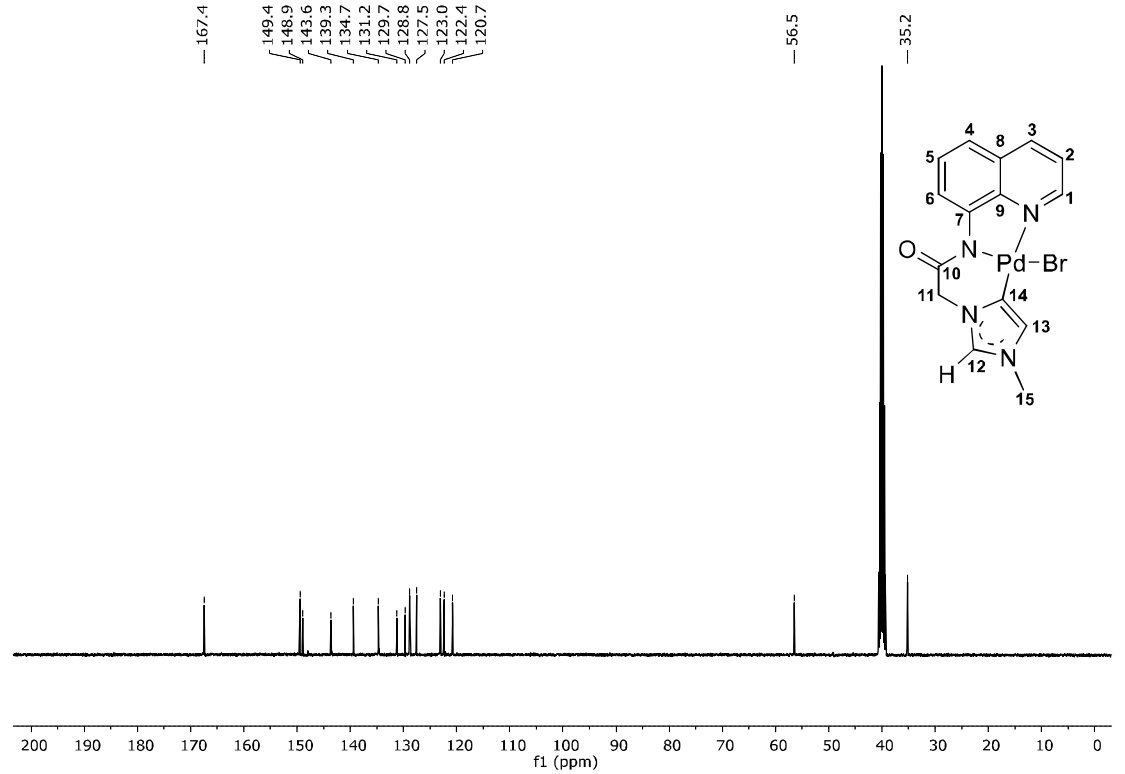

Figure 4.12 ^{13}C NMR spectrum of **L2PdBr** (DMSO-d_6)

^{1}H-^{1}H COSY spectrum (**Figure 4.13**) displayed scalar couplings for adjacent protons H1↔H2, H2↔H3 and H5↔H6 of quinoline moiety, however, it was difficult to locate H4↔H5 coupling due to merged resonances. Further, the connection of these six protons with their parent carbons C1 (149.4 ppm), C2 (122.3 ppm), C3 (139.3 ppm), C4 (128.4 ppm), C5 (120.7 ppm) and C6 (123.0 ppm) was confirmed by direct couplings in HSQC spectrum (**Figure 4.14**). The connection of protons H12 to C12 (134.7 ppm) and H13 to C13 (127.5 ppm) of imidazolium moiety was confirmed by the HMBC spectrum (**Figure 4.15**). The disappearance of resonances of C10 (167.4 ppm), C7 (148.92 ppm), C9 (143.64) ppm, C14 (131.2 ppm) and C8 (129.6 ppm) in the DEPT-135 spectrum confirmed the presence of five quaternary carbon atoms (**Figure 4.16**). The assignments to all protons and carbons of **L2PdBr** predicted from 1D (^{1}H, ^{13}C and DEPT-135) and 2D (COSY, HSQC and HMBC) NMR data are shown in **Table 4.1**

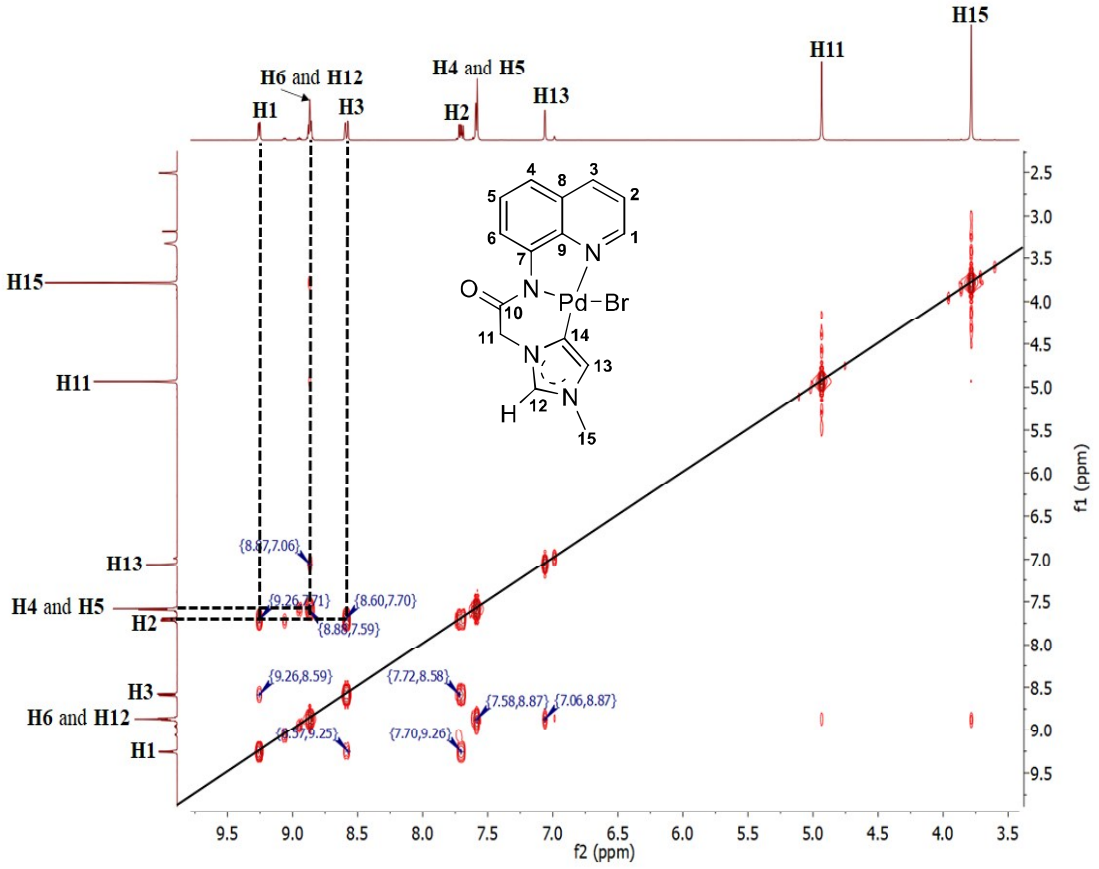

Figure 4.13 COSY spectrum of **L2PdBr** (DMSO-d_6)

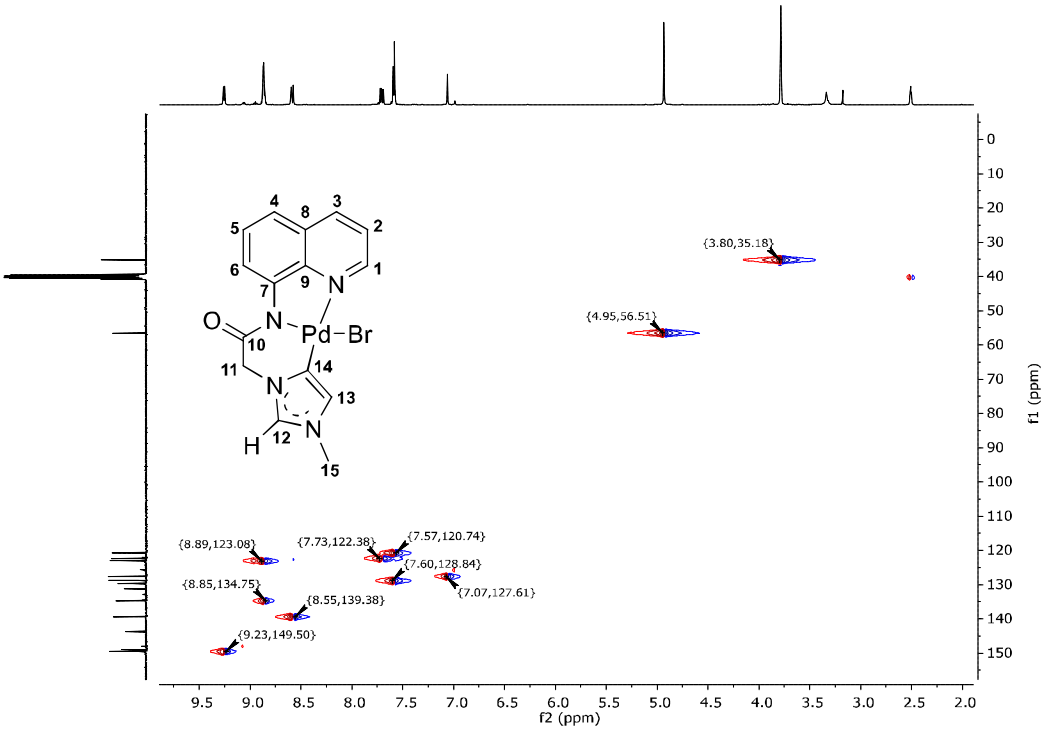

Figure 4.14 HSQC NMR spectrum of **L2PdBr** (DMSO-d_6)

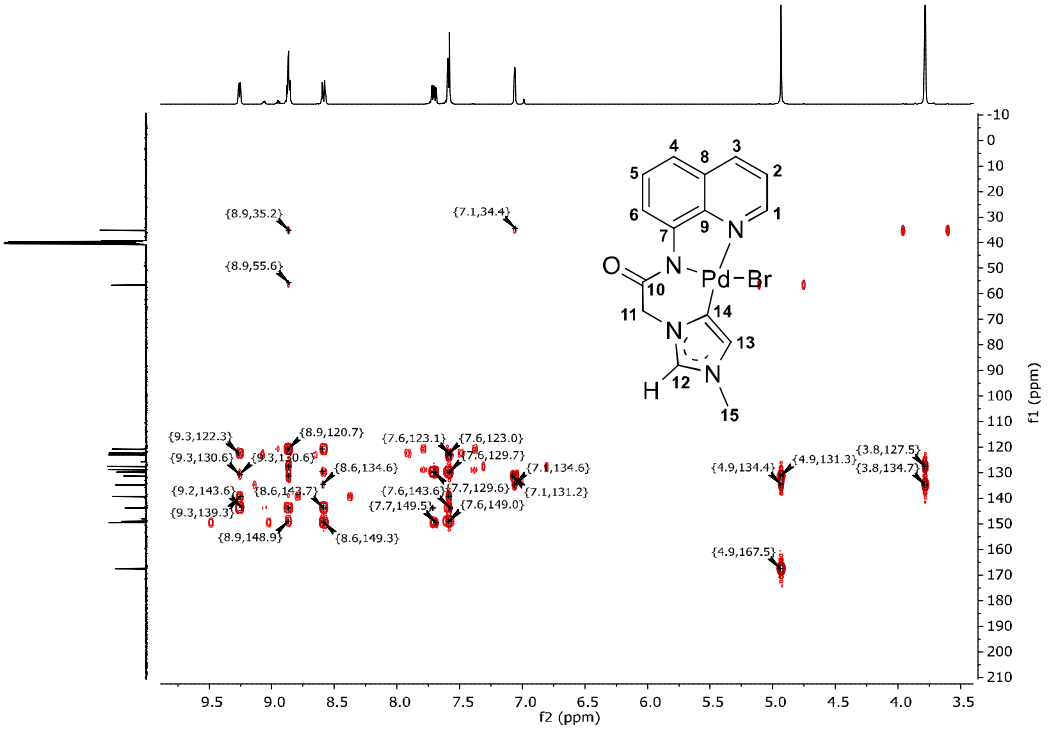

Figure 4.15 HMBC NMR spectrum of **L2PdBr** (DMSO-d_6)

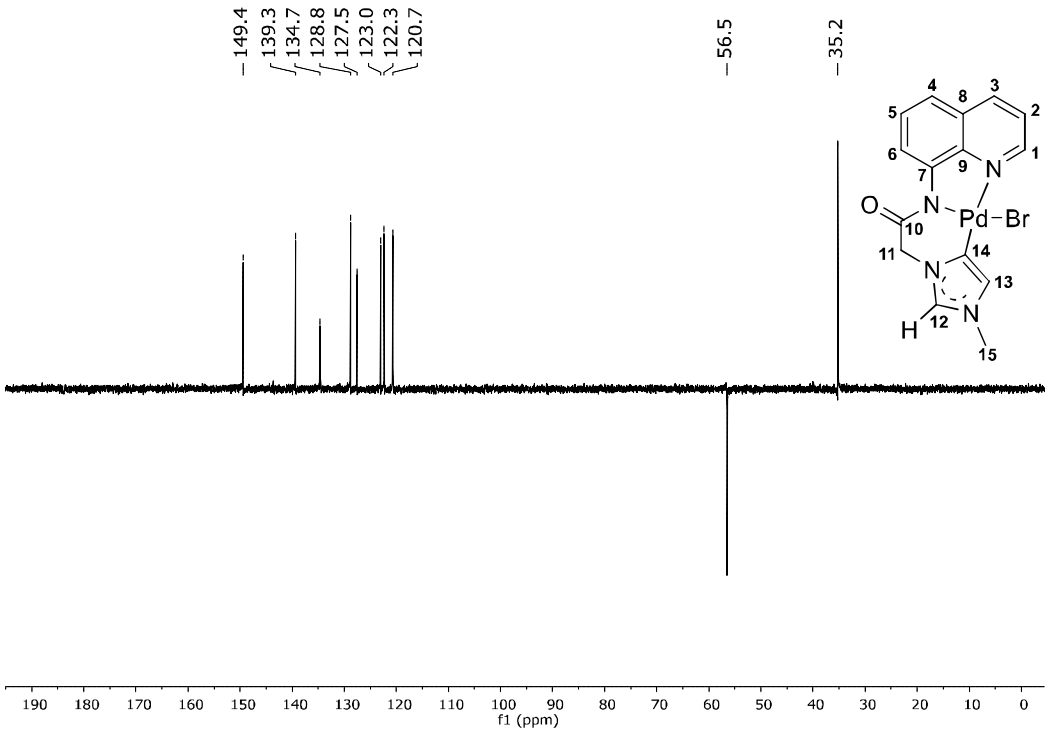

Figure 4.16 DEPT NMR spectrum of **L2PdBr** (DMSO-d_6)

Table 4.1 ^{1}H and ^{13}C chemical shifts of **L2PdBr**

Proton	Chemical shift (ppm)	Carbon	Chemical shift
H1	δ 9.26 (dd, J = 4.9, 1.4 Hz, 1H),	C1	149.4
H2	7.70 (dd, *J* = 8.3, 4.9 Hz, 1H)	C2	122.4
H3	8.58 (dd, *J* = 8.3, 1.4 Hz, 1H)	C3	139.3
H4-H5	7.60-7.56 (m, 2H)	C4	128.8
		C5	120.7
H6-H12	8.89-8.85 (m, 2H)	C6	123.0
		C12	134.7
H7	-	C7	148.9
H8	-	C8	129.7
H9	-	C9	143.6
H10	-	C10	167.4
H11	4.93 (s, 2H)	C11	56.5
H13	7.06 (d, *J* = 1.5 Hz, 1H)	C13	127.5
H14	-	C14	131.2
H15	3.78 (s, 3H)	C15	35.2

The coordination of C14 with Pd(II) in **L2PdBr** was further confirmed by single-crystal structure analysis. The single-crystal of **L2PdBr** was obtained from the DMSO-acetonitrile solvent mixture. The compound **L2PdBr** with the molecular formula $C_{15}H_{13}BrN_4OPd$ crystallized in the triclinic *P*-1 space group. The single-crystal XRD data and cell parameters are summarized in **Table 4.2**. The ORTEP diagrams of **L2PdBr** is illustrated in **Figure 4.17**. Two molecules of **L2PdBr** were found in unit cell packing (**Figure 4.18**).

Table 4.2 Crystal data and structure refinement for **L2PdBr**

Identification code	**L2PdBr**
Empirical formula	$C_{15}H_{13}BrN_4OPd$
Formula weight	451.60
Temperature/K	293
Crystal system	Triclinic
Space group	*P*-1
a/Å	7.3794(5)
b/Å	8.0408(5)
c/Å	13.4452(8)
α/°	94.425(5)
β/°	105.428(5)
γ/°	110.031(5)
Volume/Å^3	709.94(8)
Z	2
ρ_{calc}g/cm^3	2.113
μ/mm^{-1}	4.128
F(000)	440.0
Crystal size/mm^3	0.5 × 0.2 × 0.1
Radiation	MoKα (λ = 0.71073)
2Θ range for data collection/°	9.666 to 50
Index ranges	$-8 \le h \le 8$, $-9 \le k \le 9$, $-15 \le l \le 15$
Reflections collected	8257
Independent reflections	2481 [R_{int} = 0.0366, R_{sigma} = 0.0248]
Data/restraints/parameters	2481/0/195
Goodness-of-fit on F^2	1.151
Final *R* indexes [I>=2σ (I)]	$R_1{}^a$ = 0.0811, $wR_2{}^b$ = 0.1966
Final *R* indexes [all data]	$R_1{}^a$ = 0.0857, $R_2{}^b$ = 0.2057
Largest diff. peak/hole / e Å^{-3}	2.02/-3.71

[a] $R_1 = \sum||F_o| - |F_c||/\sum|F_o|$. [b] $wR_2 = [\sum w(F_o^2 - F_c^2)^2/\sum w(F_o^2)^2]^{1/2}$, where $w = 1/[\sigma^2(F_o^2) + (aP)^2 + bP]$, $P = (F_o^2 + 2F_c^2)/3$.

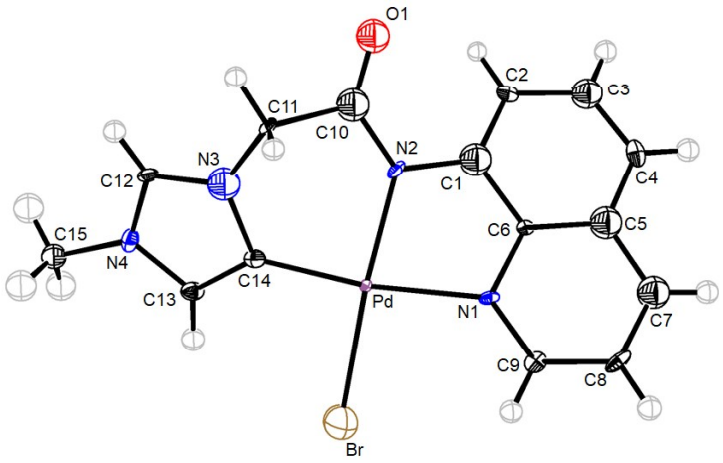

Figure 4.17 ORTEP diagram of **L2PdBr** is drawn with a 50 % ellipsoidal probability

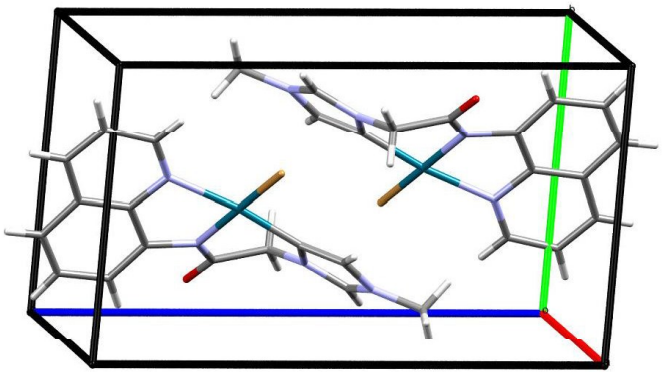

Figure 4.18 Unit cell packing of **L2PdBr**

All the calculated bond lengths and bond angles of **L2PdBr** are given in **Table 4.3** and **Table 4.4**. The Pd(1)–C(14), Pd(1)–N(1), Pd(1)–N(2) and Pd(1)–Br(1) bond lengths are 1.943(13), 2.077(10), 2.004(10) and 2.378(2) Å, respectively. The C(13)–C(14)–N3, C(14)–Pd(1)–N(1), C(14)–Pd(1)–N(2) and N(1)–Pd(1)–N2 bond angles are 103.0(11)°, 171.9(5)°, 91.6(5)° and 80.6(4)°, respectively. The bond lengths and the bond angles are in good agreement with the previously reported palladium aNHC complexes [51, 60-61].

Table 4.3 Bond Lengths for **L2PdBr**

Atom	Length/Å	Atom	Length/Å
Pd(1)–Br(1)	2.378(2)	C(10)–C(11)	1.535(17)
Pd(1)–N(1)	2.077(10)	N(4)–C(12)	1.339(17)
Pd(1)–N(2)	2.004(10)	N(4)–C(13)	1.376(17)

Pd(1)–C(14)	1.943(13)	N(4)–C(15)	1.448(17)
N(1)–C(9)	1.320(16)	C(9)–C(8)	1.388(19)
N(1)–C(6)	1.378(16)	C(3)–C(4)	1.360(19)
N(2)–C(10)	1.359(16)	C(3)–C(2)	1.412(18)
N(2)–C(1)	1.406(16)	C(6)–C(1)	1.434(16)
O(1)–C(10)	1.207(16)	C(6)–C(5)	1.393(17)
N(3)–C(14)	1.420(16)	C(1)–C(2)	1.386(18)
N(3)–C(12)	1.334(17)	C(4)–C(5)	1.414(19)
N(3)–C(11)	1.465(16)	C(8)–C(7)	1.38(2)
C(14)–C(13)	1.376(18)	C(5)–C(7)	1.429(18)

Table 4.4 Bond Angles for **L2PdBr**

Atoms	**Angle/°**	**Atom**	**Angle/°**
N(1)–Pd(1)–Br(1)	95.7(3)	C(12)–N(4)–C(13)	109.4(11)
N(2)–Pd(1)–Br(1)	172.0(3)	C(12)–N(4)–C(15)	124.4(11)
N(2)–Pd(1)–N(1)	80.6(4)	C(13)–N(4)–C(15)	125.7(11)
C(14)–Pd(1)–Br(1)	91.7(4)	N(1)–C(9)–C(8)	123.7(12)
C(14)–Pd(1)–N(1)	171.9(5)	C(4)–C(3)–C(2)	123.0(12)
C(14)–Pd(1)–N(2)	91.6(5)	N(1)–C(6)–C(1)	116.1(11)
C(9)–N(1)–Pd(1)	131.2(9)	N(1)–C(6)–C(5)	122.8(11)
C(9)–N(1)–C(6)	117.6(11)	C(5)–C(6)–C(1)	121.0(11)
C(6)–N(1)–Pd(1)	110.4(8)	N(2)–C(1)–C(6)	115.1(11)
C(10)–N(2)–Pd(1)	128.7(9)	C(2)–C(1)–N(2)	127.2(11)
C(10)–N(2)–C(1)	119.9(10)	C(2)–C(1)–C(6)	117.6(11)
C(1)–N(2)–Pd(1)	111.2(8)	C(3)–C(4)–C(5)	118.2(12)
C(14)–N(3)–C(11)	123.8(10)	C(7)–C(8)–C(9)	119.6(12)
C(12)–N(3)–C(14)	111.3(10)	N(3)–C(12)–N(4)	107.1(11)
C(12)–N(3)–C(11)	124.6(10)	C(1)–C(2)–C(3)	119.8(12)
N(3)–C(14)–Pd(1)	119.6(9)	N(4)–C(13)–C(14)	109.2(11)

C(13)–C(14)–Pd(1)	137.3(10)	C(6)–C(5)–C(4)	120.0(12)
C(13)–C(14)–N(3)	103.0(11)	C(6)–C(5)–C(7)	117.4(11)
N(2)–C(10)–C(11)	113.8(11)	C(4)–C(5)–C(7)	122.5(12)
O(1)–C(10)–N(2)	128.0(11)	N(3)–C(11)–C(10)	115.1(10)
O(1)–C(10)–C(11)	118.0(11)	C(8)–C(7)–C(5)	118.6(11)

HRMS data showed the presence of [**L2H** - Br]$^+$ at *m/z* = 267.1319 (267.1240, calculated) and [**L2PdBr** - Br]$^+$ at *m/z* = 371.0122 (371.0124, calculated) (**Figure 4.19** and **Figure 4.20**).

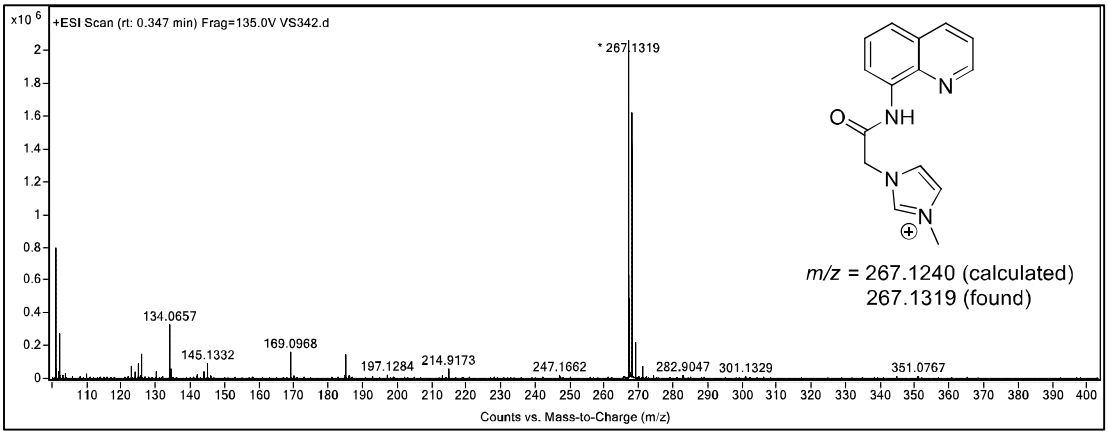

Figure 4.19 HRMS of **L2H**

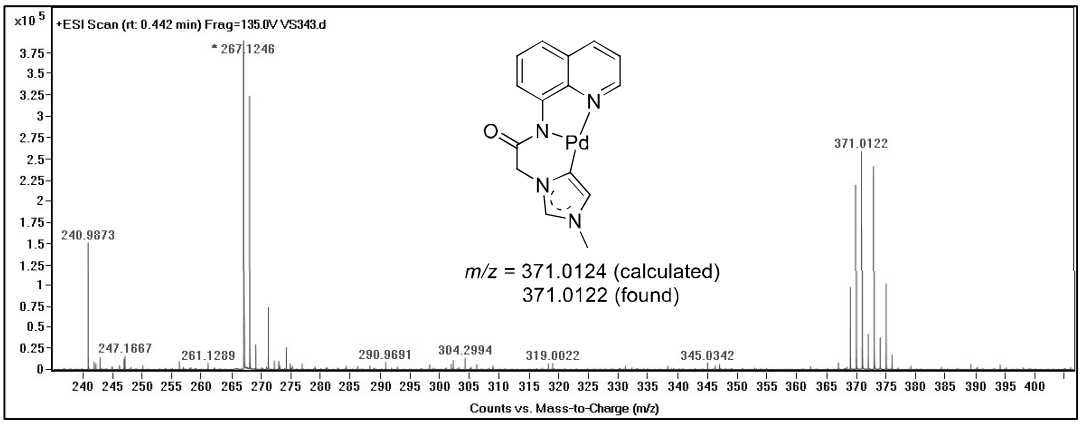

Figure. 4.20 HRMS of **L2PdBr**

4.2.2 Catalytic application of L2PdBr in the Suzuki-Miyaura cross-coupling

The catalytic ability of complex **L2PdBr** for the Suzuki-Miyaura cross-coupling was investigated. Extensive screening of different bases, solvents, temperature, catalyst, and base loading was performed using *p*-chlorotoluene (**17b**) and phenylboronic acid (**18a**) as substrates

under microwave irradiation (**Table 4.5**). The investigation initiated by choosing H_2O as a solvent system, using 1 mol% **L2PdBr** and 3 equiv. of K_2CO_3, provided biaryl product **19b** in 92% yield (**Table 4.5**, entry 1). Among different bases, K_2CO_3 showed better results (**Table 4.5**, entries 1-10). The effect of the solvents using K_2CO_3 as the base was also investigated (**Table 4.5**, entries 1, 11-14). **19b** was obtained in high yields in DMF, H_2O, and EtOH, low yield in ACN and no product formation was observed in toluene. Increasing or lowering the amount of **L2PdBr** from 1 mol% resulted in a decreased yield of **19b** (**Table 4.5**, entries 1, 15-17). Further increasing the K_2CO_3 amount from 1.0 to 3.0 equiv. improved the product yield (**Table 4.5**, entries 1, 18-21). Finally, the effect of the temperature was evaluated, and lower yields were obtained upon increasing or decreasing the reaction temperature from 120 °C (**Table 4.5**, entries 22 and 23). 1 mol% of **L2PdBr**, 3 equiv. of K_2CO_3 at 120 °C and use of green solvent H_2O under microwave irradiation for 15 min was chosen as the optimized reaction conditions for biaryl formation.

Table 4.5 Optimization of the Suzuki-Miyaura cross-coupling reaction

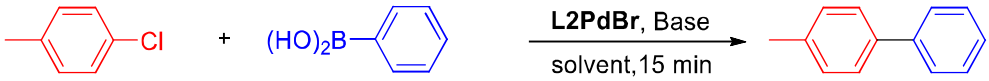

17b **18a** **19b**

Entry	L2PdBr (mol%)	Base (equiv.)	Solvent	Yield (%)[b]
1	**1**	**K_2CO_3 (3)**	**H_2O**	**92**
2	1	Na_2CO_3 (3)	H_2O	71
3	1	Cs_2CO_3 (3)	H_2O	36
4	1	NaOH (3)	H_2O	trace
5	1	KOH (3)	H_2O	30
6	1	KO^{t}Bu (3)	H_2O	60
7	1	K_3PO_4 (3)	H_2O	40
8	1	$KHCO_3$ (3)	H_2O	trace
9	1	$NaHCO_3$ (3)	H_2O	57
10	1	NEt_3 (3)	H_2O	-
11	1	K_2CO_3 (3)	DMF	93
12	1	K_2CO_3 (3)	EtOH	90
13	1	K_2CO_3 (3)	CH_3CN	20

14	1	K_2CO_3 (3)	Toluene	-
15	3	K_2CO_3 (3)	H_2O	90
16	0.5	K_2CO_3 (3)	H_2O	87
17	0.1	K_2CO_3 (3)	H_2O	76
18	1	K_2CO_3 (1)	H_2O	79
19	1	K_2CO_3 (1.5)	H_2O	83
20	1	K_2CO_3 (2)	H_2O	88
21	1	K_2CO_3 (2.5)	H_2O	90
22[c]	1	K_2CO_3 (3)	H_2O	84
23[d]	1	K_2CO_3 (3)	H_2O	69

[a]Reaction conditions: **17b** (1 mmol), **18a** (1.2 mmol). [b]isolated yield. [c]temp. at 110 °C. [d]temp. at 130 °C.

Due to the remarkable activity of **L2PdBr**, we further expanded the coupling reaction of various aryl chlorides (chlorobenzene, *p*-chlorotoluene, *p*-nitrochlorobenzene, *p*-chloroacetophenone, *p*-chloroanisole, *o*-chlorotoluene, *o*-aminochlorobenzene, *o*-chloroanisole, and *o*-nitrochlorobenzene) with different boronic acids (phenylboronic acid, *p*-methoxyboronic acid, *o*-methylboronic acid, napthene-1-boronic acid, 3,4-dimethoxyboronic acid, 2,3,4-trimethoxyboronic acid, 3,4,5-trimethoxyboronic acid, and phenanthrene-9-boronic acid) under optimized reaction condition (**Table 4.6**). Aryl chlorides and boronic acid with electron-neutral, electron-donating, and electron-withdrawing groups at *para* position gave the biaryl product in 95-82% yields (**Table 4.6**, entries **19a**, **19b**, **19c**, **19d**, **19h 19i**, and **19j**). The *ortho*-substituted aryl halides and boronic acids were also tolerated under these reaction conditions (**Table 4.6**, entries **19e**, **19f, 19g**, **19k,** and **19l**). Sterically hindered and bulky boronic acid derivatives (**Table 4.6**, entries **19m-t**) reacted well and provided the desired product in good yields. Encouraged by the good catalytic applicability of **L2PdBr**, we extended this protocol for the synthesis of more challenging heteroaryls by increasing reaction time to 30 mins. Heteroaryl chlorides (2-chloropyridine, 2-chloropyrazine, and 2,6-dichloropyrazine) reacted well with arylboronic acid derivatives and provided mono and biheteroarylated products in satisfactory yields (**Table 4.6**, entries **19u-y**). All the synthesized compounds were isolated by column chromatography and characterized by ^{1}H and ^{13}C NMR spectroscopy. The representative ^{1}H and ^{13}C NMR spectra of **19b** are shown in **Figure 4.21** and **Figure 4.22**.

Table 4.6 The Suzuki-Miyaura coupling reaction of aryl chlorides with arylboronic acids[a]

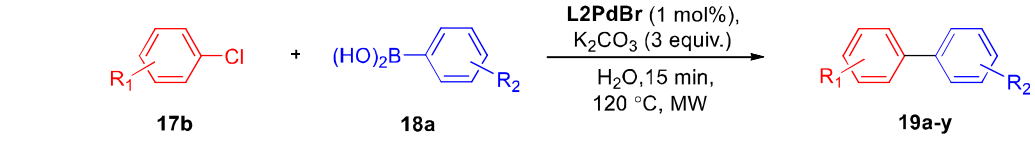

17b + 18a → 19a-y

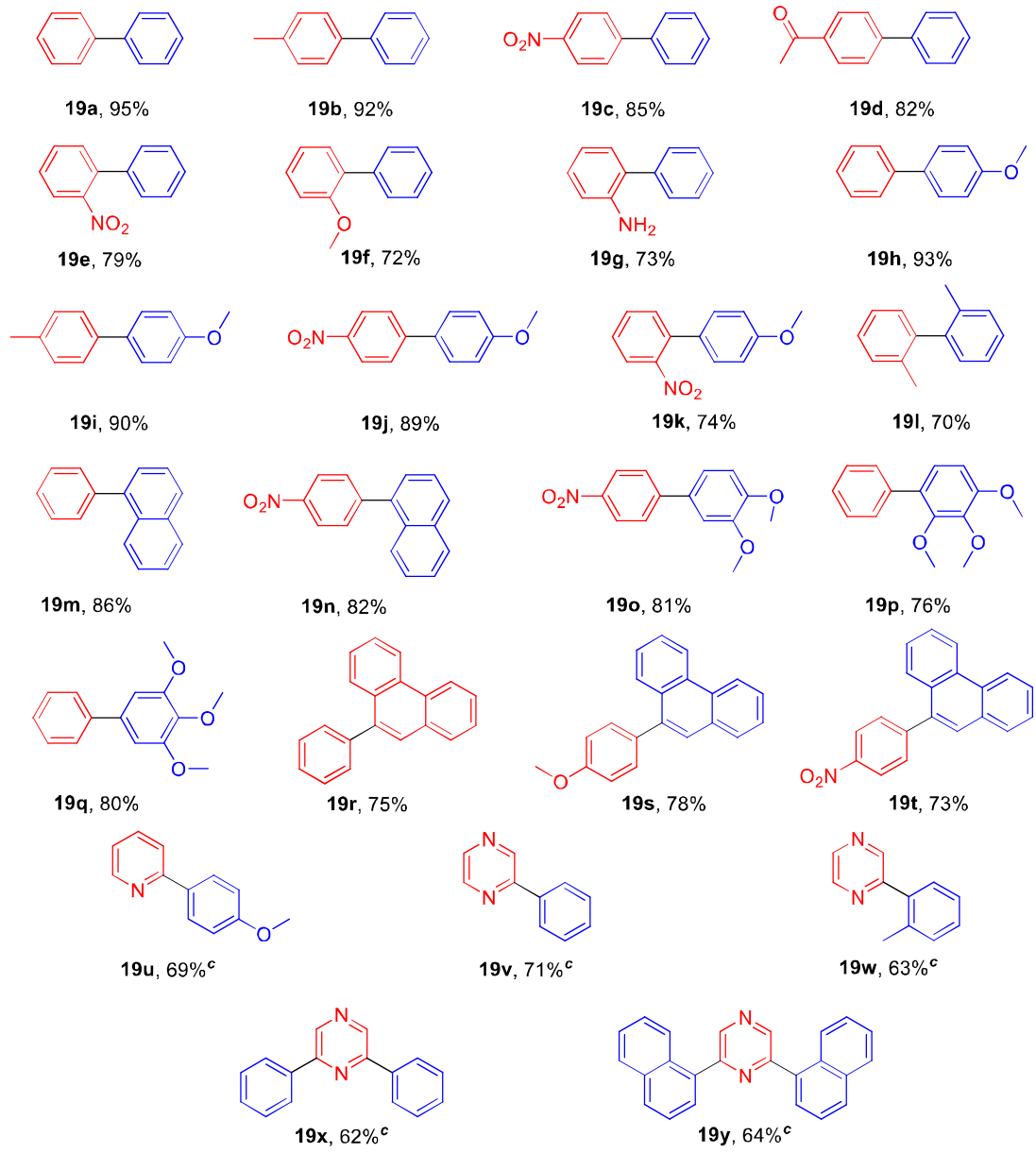

[a]Reaction conditions: aryl halide (1.0 mmol), boronic acid (1.2 mmol), K_2CO_3 (3.0 equiv.), and 3 mL H_2O. [b]Yield. [c]Time: 30 mins.

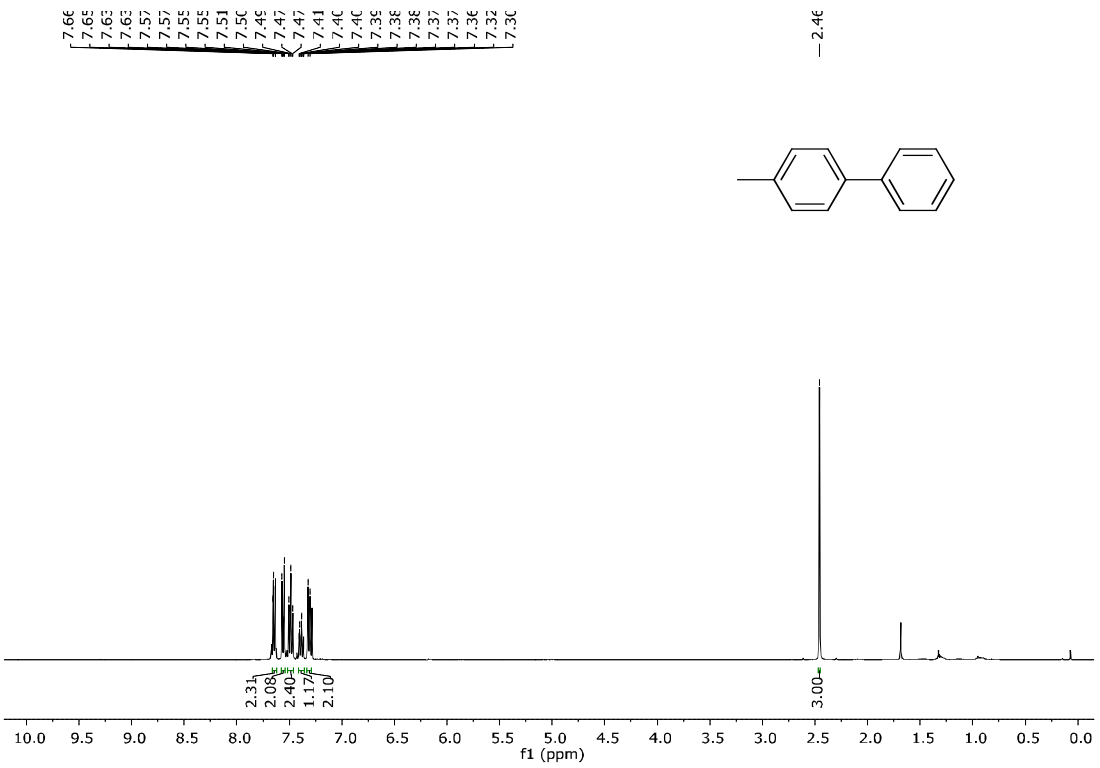

Figure 4.21 ^{1}H NMR spectrum of **19b** ($CDCl_3$)

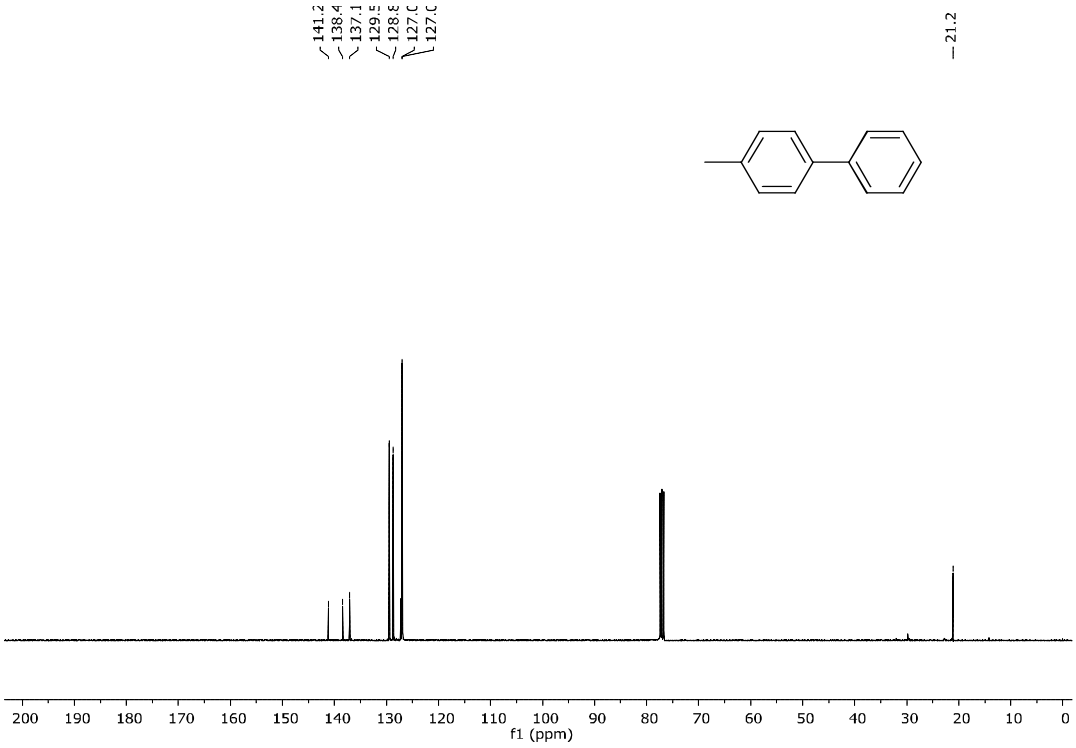

Figure 4.22 ^{13}C NMR spectrum of **19b** ($CDCl_3$)

4.2.3 Mechanism of the Suzuki-Miyaura cross-coupling reaction

To study the possible mechanism for this transformation, the coupling of **17b** with **18a** in the presence of K_2CO_3 in H_2O was monitored by electrospray ionization high-resolution mass spectrometry (ESI-HRMS). The proposed plausible mechanism is shown in **Scheme 4.3**.

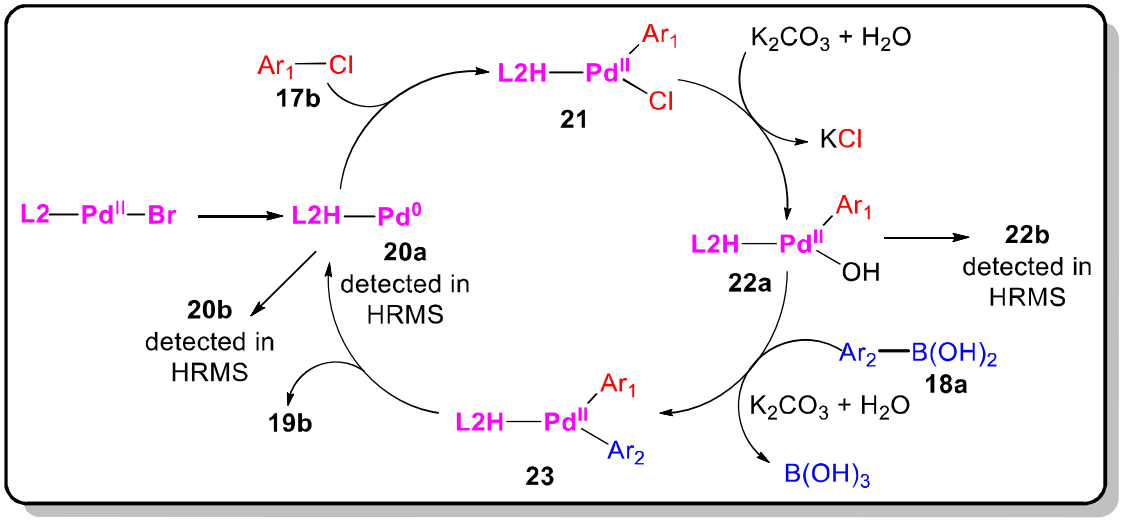

Scheme 4.3 Plausible mechanism and reactive intermediates identified by ESI-HRMS

In mass spectrum, the characteristic isotopic pattern of palladium suggests the presence of active Pd(0) species **20a** at *m/z* 444.0643 (calcd for $C_{15}H_{22}N_4O_5Pd^+$ ([**L2HPd** + $4H_2O$ - Br]$^+$): 444.0620) [62]. Another mass pattern at *m/z* 412.0383 for Pd(0) species **20b** (calcd for $C_{14}H_{18}N_4O_4Pd^+$ ([**20a** + H - H_2O - CH_3]$^+$): 412.0363), indicates the removal of water molecule and methyl group from **20a** during ionization (**Figure 4.23**).

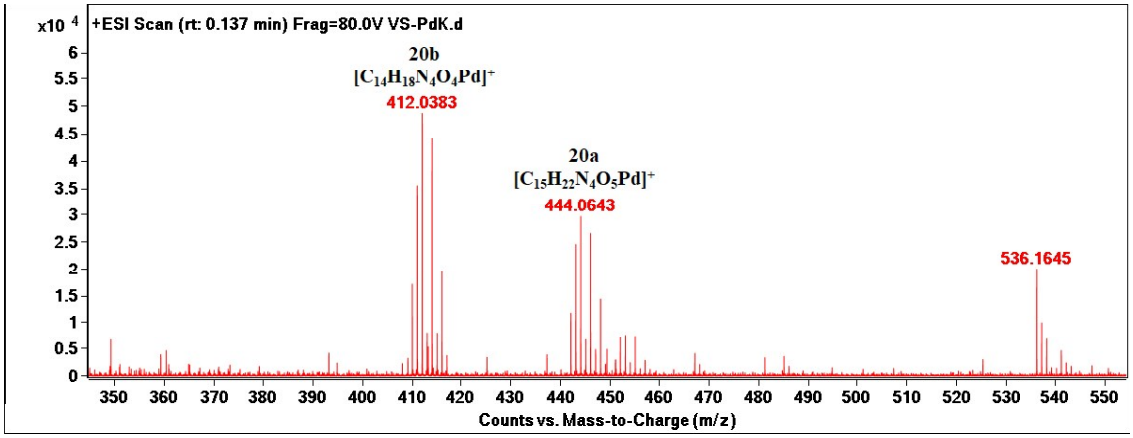

Figure 4.23 HRMS of **20a** and **20b**

Next, the oxidative addition of aryl halide **17b** to **20a** gives **21**. The Cl^- ligand exchange reaction in **21** by OH^- results in the formation of **22a** [63]. A prominent peak observed for **22b** at *m/z* 465.0659 (calcd for $C_{21}H_{19}N_4O_2Pd^{+\bullet}$ ([**22a** - CH_3]$^{+\bullet}$): 465.0543) indicates the rapid ionization of **22a** to **22b** (**Figure 4.24**). In the next step, transmetalation of **22a** with **18a** gives **23**, and finally, on reductive elimination, the cross-coupled product **19b** is formed and **20a** is regenerated.

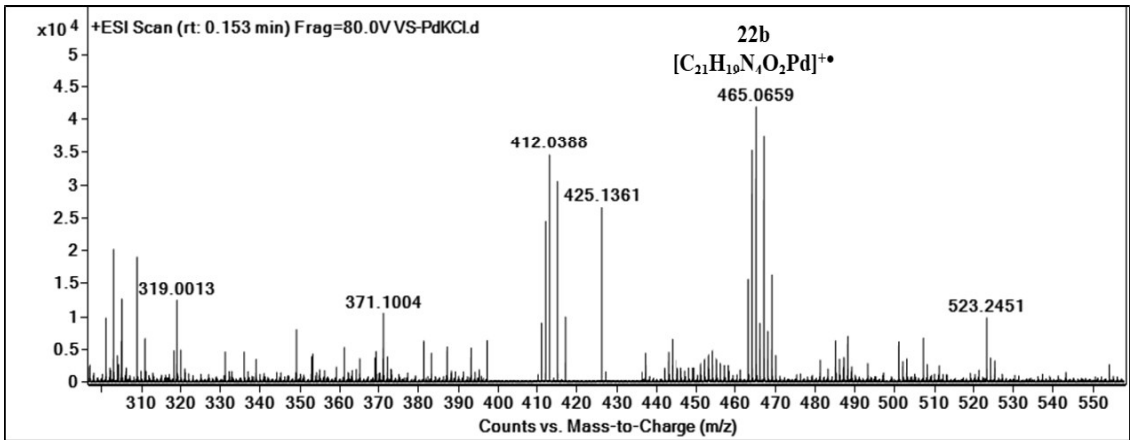

Figure 4.24 HRMS of **22b**

4.3 Experimental

4.3.1 Synthesis of 2-bromo-N-(quinolin-8-yl)acetamide

To a stirred solution of bromoacetic acid (1 mmol) in dioxane at 0 °C, ethyl chloroformate (1 mmol) and triethylamine (1 mmol) were added. After 40 min, 8-aminoquinoline (1 mmol) was added and the reaction mixture was kept at room temperature till the completion of the reaction. Dioxane was evaporated under vacuum on a rotary evaporator, the residue was diluted with water and the product was extracted in ethyl acetate. The ethyl acetate layer was washed with water, dried over anhydrous sodium sulfate, and evaporated under reduced pressure. The crude product was purified by column chromatography using hexanes and ethyl acetate as the eluent to afford 2-bromo-N-(quinolin-8-yl)acetamide (**Scheme 4.2**).

4.3.2 Synthesis of imidazolium-based ligand L2H

2-bromo-N-(quinolin-8-yl)acetamide (discussed in chapter 2, section 2.4) (1 mmol) and 1-methylimidazole (1.2 mmol) was stirred at 70 ^oC for 6 hr. Obtained crude was washed with ethyl acetate and ether to give **L2H** (**Scheme 4.2**).

4.3.3 Synthesis of imidazolium-based NHC/CNN pincer palladium(II) complex L2PdBr

L2H (2 mmol) was dissolved in methanol and to this solution $Pd(OAc)_2$ (1 mmol) was added, the reaction mixture was stirred for 5 h at 70 °C. A precipitate was isolated by filtration, washed with ethyl acetate and ether, dried under vacuum to afford complex **L2PdBr** as a yellowish green powder (**Scheme 4.2**).

4.3.4 General procedure for the Suzuki-Miyaura reaction

A mixture of aryl chloride (1 mmol), boronic acid (1.2 mmol), K_2CO_3 (3 equiv.) and **L2PdBr** (1 mol%) in 3 mL H_2O was stirred under microwave irradiation at 120 °C for 15 min. After completion, the reaction mixture was cooled down to room temperature and product was extracted in ethyl acetate. The ethyl acetate layer was washed with water, dried over anhydrous sodium sulfate and evaporated under reduced pressure. The crude product was purified by column chromatography using a mixture of hexanes and ethyl acetate as the eluent.

4.3.5 Physical and spectral data of synthesized compounds

2-bromo-N-(quinolin-8-yl)acetamide

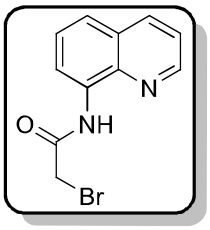

White solid (71%); mp: 128-129 °C; ^{1}H NMR (400 MHz, $CDCl_3$) δ 10.93 (s, 1H), 8.88 (dd, *J* = 4.2, 1.6 Hz, 1H), 8.81-8.74 (m, 1H), 8.19 (dd, *J* = 8.3, 1.6 Hz, 1H), 7.64-7.54 (m, 2H), 7.50 (dd, *J* = 8.3, 4.2 Hz, 1H), 4.34 (s, 2H). ^{13}C NMR (100 MHz, $CDCl_3$) δ 164.4, 148.7, 138.8, 136.3, 133.6, 128.0, 127.2, 122.5, 121.8, 116.6, 29.7.

3-methyl-1-(2-oxo-2-(quinolin-8-ylamino)ethyl)-1H-imidazol-3-ium bromide (L2H)

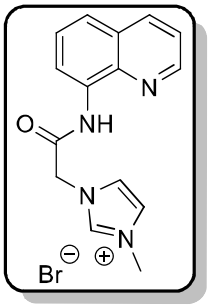

Pale brown solid (96%); mp: 107-108 °C; ^{1}H NMR (400 MHz, DMSO-d_6) δ 10.89 (s, 1H), 9.23 (s, 1H), 9.00 (dd, *J* = 4.2, 1.5 Hz, 1H), 8.59-8.44 (m, 2H), 7.83 (s, 1H), 7.78 (s, 1H), 7.77-7.73 (m, 1H), 7.69 (dd, *J* = 8.3, 4.2 Hz, 1H), 7.61 (t, *J* = 8.0 Hz, 1H), 5.52 (s, 2H), 3.95 (s, 3H); ^{13}C NMR (100 MHz, DMSO-d_6) δ 165.1, 149.6, 138.8, 138.4, 137.2, 134.5, 128.4, 127.3, 124.3, 123.6, 123.3, 122.8, 118.0, 52.2, 36.4. HRMS (ESI): *m/z* calcd for $[C_{15}H_{15}N_4O]^+$ [**L2H** - Br]$^+$ 267.1240, found 267.1319.

Abnormal NHC/CNN pincer palladium(II) complex (L2PdBr)

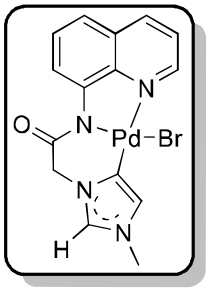

Yellowish green solid (65%); mp: 263-264 °C; ^{1}H NMR (400 MHz, DMSO-d_6) δ 9.26 (dd, J = 4.9, 1.4 Hz, 1H), 8.89-8.85 (m, 2H), 8.58 (dd, *J* = 8.3, 1.4 Hz, 1H), 7.70 (dd, *J* = 8.3, 4.9 Hz, 1H), 7.60-7.56 (m, 2H), 7.06 (d, *J* = 1.5 Hz, 1H), 4.93 (s, 2H), 3.78 (s, 3H); ^{13}C NMR (100 MHz, DMSO-d_6) δ 167.4, 149.4, 148.9, 143.6, 139.3, 134.7, 131.2, 129.7, 128.8, 127.5, 123.0, 122.4, 120.7, 56.5, 35.2. HRMS (ESI): *m/z* calcd for $[C_{15}H_{13}N_4OPd]^+$ [**L2PdBr** - Br]$^+$ 371.0124, found 371.0122).

^{1}H NMR and ^{13}C NMR Spectral data of the Suzuki-Miyaura coupling products

1,1'-biphenyl (19a)

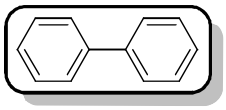

White solid; ^{1}H NMR (400 MHz, $CDCl_3$) δ 7.66-7.62 (m, 4H), 7.51-7.46 (m, 4H), 7.42-7.36 (m, 2H); ^{13}C NMR (100 MHz, $CDCl_3$) δ 141.2, 128.8, 127.3, 127.2.

4-methyl-1,1'-biphenyl (19b)

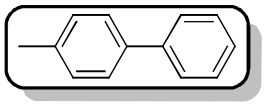

White solid; ^{1}H NMR (400 MHz, $CDCl_3$) δ 7.64 (dd, *J* = 8.2, 1.2 Hz, 2H), 7.58-7.54 (m, 2H), 7.51-7.46 (m, 2H), 7.41-7.36 (m, 1H), 7.31 (d, *J* = 7.9 Hz, 2H), 2.46 (s, 3H); ^{13}C NMR (100 MHz, $CDCl_3$) δ 141.2, 138.4, 137.1, 129.5, 128.8, 127.0, 127.0, 21.2.

4-nitro-1,1'-biphenyl (19c)

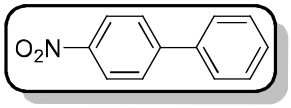

Pale yellow solid; ^{1}H NMR (400 MHz, $CDCl_3$) δ 8.36-8.30 (m, 2H), 7.79-7.74 (m, 2H), 7.68-7.63 (m, 2H), 7.56-7.45 (m, 3H); ^{13}C NMR (100 MHz, $CDCl_3$) δ 147.6, 147.1, 138.8, 129.2, 128.9, 127.8, 127.4, 124.1.

1-([1,1'-biphenyl]-4-yl)ethan-1-one (19d)

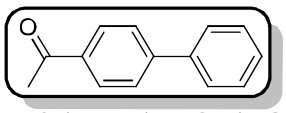

White solid; ^{1}H NMR (400 MHz, $CDCl_3$) δ 8.08-8.04 (m, 2H), 7.74-7.70 (m, 2H), 7.66 (m, *J* = 7.0, 1.5 Hz, 2H), 7.53-7.48 (m, 2H), 7.46-7.40 (m, 1H), 2.67 (s, 3H); ^{13}C NMR (100 MHz, $CDCl_3$) δ 197.7, 145.8, 139.9, 135.9, 129.0, 128.9, 128.2, 127.3, 127.2, 26.6.

2-nitro-1,1'-biphenyl (19e)

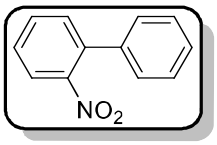

Yellow solid; ^{1}H NMR (400 MHz, $CDCl_3$) δ 7.88 (dd, *J* = 8.1, 1.2 Hz, 1H), 7.65 (td, *J* = 7.6, 1.3 Hz, 1H), 7.54-7.43 (m, 5H), 7.36 (dd, *J* = 7.6, 1.9 Hz, 2H); ^{13}C NMR (100 MHz, $CDCl_3$) δ 149.3, 137.4, 136.3, 132.3, 132.0, 128.7, 128.3, 128.2, 127.9, 124.1.

2-methoxy-1,1'-biphenyl (19f)

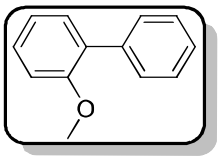

Colourless oil; ^{1}H NMR (400 MHz, $CDCl_3$) δ 7.58-7.53 (m, 2H), 7.44 (t, *J* = 7.5 Hz, 2H), 7.35 (td, *J* = 5.7, 1.4 Hz, 3H), 7.09-7.00 (m, 2H), 3.84 (s, 3H); ^{13}C NMR (100 MHz, $CDCl_3$) δ 156.4, 138.5, 130.9, 129.5, 128.6, 128.0, 126.9, 120.8, 111.2, 55.6.

[1,1'-biphenyl]-2-amine (19g)

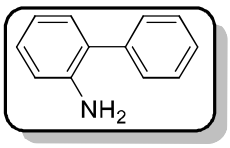

Pale brown solid; ^{1}H NMR (400 MHz, $CDCl_3$) δ) 7.54-7.45 (m, 4H), 7.43-7.37 (m, 1H), 7.25-7.17 (m, 2H), 6.89 (td, *J* = 7.5, 1.1 Hz, 1H), 6.82 (dd, *J* = 7.9, 0.9 Hz, 1H), 3.68 (s, 2H); ^{13}C NMR (100 MHz, $CDCl_3$) δ 143.5, 139.6, 130.5, 129.1, 128.8, 128.5, 127.7, 127.2, 118.7, 115.6.

4-methoxy-1,1'-biphenyl (19h)

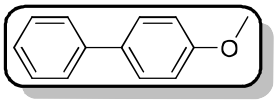

White solid; ^{1}H NMR (400 MHz, $CDCl_3$) δ 7.61-7.55 (m, 4H), 7.48-7.43 (m, 2H), 7.37-7.32 (m, 1H), 7.04-7.01 (m, 2H), 3.89 (s, 3H); ^{13}C NMR (100 MHz, $CDCl_3$) δ 159.1, 140.8, 133.8, 128.7, 128.2, 126.8, 126.7, 114.2, 55.4.

4-methoxy-4'-methyl-1,1'-biphenyl (19i)

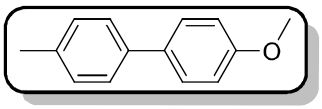

White solid; ^{1}H NMR (400 MHz, $CDCl_3$) δ 7.57-7.54 (m, 2H), 7.51-7.48 (m, 2H), 7.29-7.25 (m, 2H), 7.03-6.99 (m, 2H), 3.88 (s, 3H), 2.43 (s, 3H); ^{13}C NMR (100 MHz, $CDCl_3$) δ 159.0, 138.0, 136.4, 133.8, 129.5, 128.0, 126.6, 114.2, 55.4, 21.1.

4-methoxy-4'-nitro-1,1'-biphenyl (19j)

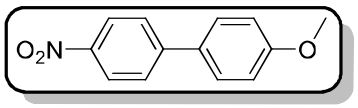

Yellow oil; ^{1}H NMR (400 MHz, $CDCl_3$) δ 8.29 (d, *J* = 8.9 Hz, 2H), 7.71 (d, *J* = 8.9 Hz, 2H), 7.61 (d, *J* = 8.8 Hz, 2H), 7.04 (d, *J* = 8.8 Hz, 2H), 3.90 (s, 3H); ^{13}C NMR (100 MHz, $CDCl_3$) δ 160.4, 147.2, 146.5, 131.1, 128.6, 127.1, 124.2, 114.6, 55.4.

4'-methoxy-2-nitro-1,1'-biphenyl (19k)

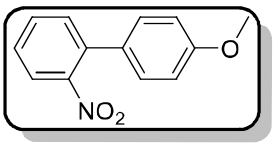

Yellow solid (74%); ^{1}H NMR (400 MHz, $CDCl_3$) δ 7.85-7.81 (m, 1H), 7.64-7.59 (m, 1H), 7.46 (t, *J* = 7.4 Hz, 2H), 7.31-7.27 (m, 2H), 7.01-6.97 (m, 2H), 3.87 (s, 3H); ^{13}C NMR (100 MHz, $CDCl_3$) δ 159.7, 149.4, 135.9, 132.2, 131.9, 129.5, 129.1, 127.8, 124.0, 114.2, 55.3.

2,2'-dimethyl-1,1'-biphenyl (19l)

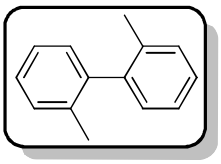

Colourless liquid; ^{1}H NMR (400 MHz, $CDCl_3$) δ 7.56-7.50 (m, 2H), 7.38 (qd, *J* = 6.7, 1.9 Hz, 6H), 2.50 (s, 6H); ^{13}C NMR (100 MHz, $CDCl_3$) δ 141.7, 136.8, 136.4, 131.1, 130.1, 129.3, 126.2, 2.

1-phenylnaphthalene (19m)

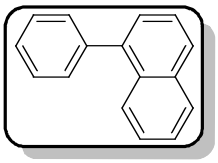

White solid; ^{1}H NMR (400 MHz, $CDCl_3$) δ 8.06-7.93 (m, 3H), 7.70-7.20 (m, 9H); ^{13}C NMR (100 MHz, $CDCl_3$) δ 138.5, 133.5, 132.8, 128.2, 127.9, 127.8, 126.6, 126.0, 125.0, 125.8, 125.4.

1-(4-nitrophenyl)naphthalene (19n)

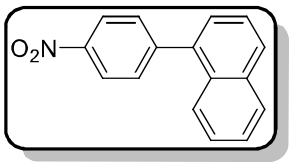

Pale yellow solid; ^{1}H NMR (400 MHz, $CDCl_3$). δ 8.39 (d, *J* = 8.8 Hz, 2H), 7.97 (dd, *J* = 7.9, 3.2 Hz, 2H), 7.82 (d, *J* = 8.6 Hz, 1H), 7.70 (d, *J* = 8.8 Hz, 2H), 7.62-7.55 (m, 2H), 7.54-7.49 (m, 1H), 7.46 (dd, *J* = 7.1, 1.1 Hz, 1H); ^{13}C NMR (100 MHz, $CDCl_3$) δ 147.7, 147.2, 137.8, 133.8, 131.0, 130.9, 129.0, 128.6, 127.1, 126.7, 126.2, 125.3, 125.1, 123.6.

3,4-dimethoxy-4'-nitro-1,1'-biphenyl (19o)

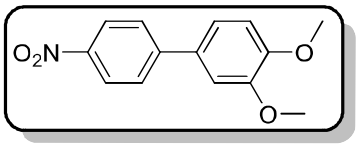

Yellow solid;^{1}H NMR (400 MHz, $CDCl_3$) δ 8.31-8.26 (m, 2H), 7.74-7.69 (m, 2H), 7.23 (dd, *J* = 8.3, 2.2 Hz, 1H), 7.15 (d, *J* = 2.2 Hz, 1H), 7.00 (d, *J* = 8.3 Hz, 1H), 3.99 (s, 3H), 3.97 (s, 3H); ^{13}C NMR (100 MHz, $CDCl_3$) δ 150.1, 149.5, 147.4, 146.7, 131.5, 127.2, 124.1, 120.1, 111.7, 110.5, 56.1, 56.1.

2,3,4-trimethoxy-1,1'-biphenyl (19p)

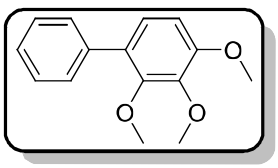

White solid; ^{1}H NMR (400 MHz, $CDCl_3$) δ 7.53 (d, *J* = 7.0 Hz, 2H), 7.46-7.41 (m, 2H), 7.34 (t, *J* = 7.3 Hz, 1H), 7.06 (d, *J* = 8.6 Hz, 1H), 6.77 (d, *J* = 8.6 Hz, 1H), 3.96 (s, 3H), 3.93 (s, 3H), 3.70 (s, 3H); ^{13}C

NMR (100 MHz, $CDCl_3$) δ 153.1, 151.4, 142.6, 138.3, 129.1, 128.8, 128.1, 126.7, 124.8, 107.5, 61.0, 60.9, 56.0.

3,4,5-trimethoxy-1,1'-biphenyl (19q)

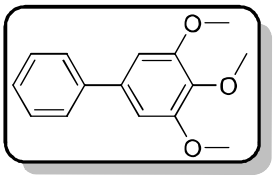

Off white solid; ^{1}H NMR (400 MHz, $CDCl_3$) δ 7.60-7.57 (m, 2H), 7.48-7.44 (m, 2H), 7.40-7.35 (m, 1H), 6.81 (s, 2H), 3.96 (s, 6H), 3.93 (s, 3H); ^{13}C NMR (100 MHz, $CDCl_3$) δ 153.5, 141.4, 137.7, 137.2, 128.7, 127.3, 127.1, 104.6, 61.0, 56.2.

9-phenylphenanthrene (19r)

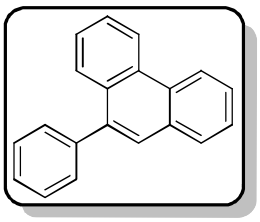

White solid; ^{1}H NMR (400 MHz, $CDCl_3$) δ 8.84 (d, *J* = 8.0 Hz, 1H), 8.79 (d, *J* = 8.1 Hz, 1H), 8.03-7.93 (m, 2H), 7.77-7.65 (m, 4H), 7.65-7.49 (m, 6H); ^{13}C NMR (100 MHz, $CDCl_3$) δ 140.9, 138.8, 131.6, 131.2, 130.1, 128.7, 127.7, 127.4, 127.0, 126.9, 126.6, 126.5, 126.5, 122.9, 122.6.

9-(4-methoxyphenyl)phenanthrene (19s)

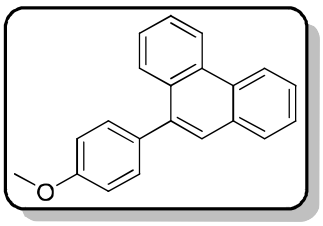

White solid; ^{1}H NMR (400 MHz, $CDCl_3$) δ 8.82 (d, *J* = 8.3 Hz, 1H), 8.76 (d, *J* = 8.1 Hz, 1H), 8.00 (d, *J* = 8.9 Hz, 1H), 7.93 (d, *J* = 9.0 Hz, 1H), 7.74-7.63 (m, 4H), 7.59 (t, *J* = 8.2 Hz, 1H), 7.54-7.50 (m, 2H), 7.12-7.08 (m, 2H), 3.95 (s, 3H); ^{13}C NMR (100 MHz, $CDCl_3$) δ 159.1, 138.4, 133.2, 131.7, 131.5, 131.1, 130.7, 129.9, 128.6, 127.5 , 127.0, 126.8, 126.5, 126.4, 122.9, 122.5, 113.8, 55.4.

9-(4-nitrophenyl)phenanthrene (19t)

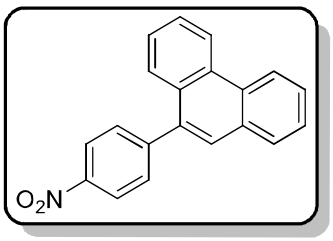

Pale yellow solid; ^{1}H NMR (400 MHz, $CDCl_3$) δ 8.83 (d, *J* = 8.4 Hz, 1H), 8.77 (d, *J* = 7.9 Hz, 1H), 8.43-8.37 (m, 2H), 7.95 (dd, *J* = 7.8, 1.5 Hz, 1H), 7.82 (dd, *J* = 8.2, 1.3 Hz, 1H), 7.78-7.66 (m, 6H), 7.60 (ddd, *J* = 8.2, 6.9, 1.2 Hz, 1H); ^{13}C NMR (100 MHz, $CDCl_3$) δ 147.8, 147.3, 136.4, 131.1, 130.9, 130.7, 130.4, 130.2, 128.9, 128.0, 127.4, 127.2, 127.0, 126.9, 126.2, 123.6, 123.2, 122.6.

2-(4-methoxyphenyl)pyridine (19u)

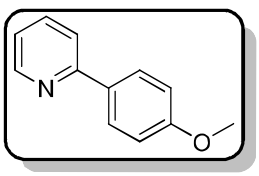

Yellow oil; ^{1}H NMR (400 MHz, $CDCl_3$) δ 8.68 (d, *J* = 4.4 Hz, 1H), 7.97 (d, *J* = 8.7 Hz, 2H), 7.72 (dt, *J* = 16.7, 7.9 Hz, 2H), 7.23-7.16 (m,

1H), 7.02 (d, *J* = 8.7 Hz, 2H), 3.89 (s, 3H); ^{13}C NMR (100 MHz, $CDCl_3$) δ 160.5, 157.1, 149.5, 136.7, 132.0, 128.2, 121.4, 119.9, 114.1, 55.4.

2-phenylpyrazine (19v)

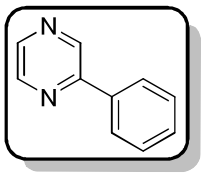

Light yellow solid; ^{1}H NMR (400 MHz, $CDCl_3$) δ 9.05 (d, *J* = 1.5 Hz, 1H), 8.65 (dd, *J* = 2.4, 1.6 Hz, 1H), 8.52 (d, *J* = 2.5 Hz, 1H), 8.06-8.00 (m, 2H), 7.56-7.46 (m, 3H); ^{13}C NMR (100 MHz, $CDCl_3$) δ 152.8, 144.2, 142.9, 142.2, 136.3, 129.9, 129.1, 126.9.

2-(o-tolyl)pyrazine (19w)

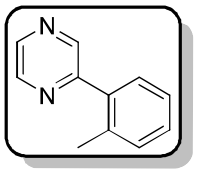

Colourless oil (63%); ^{1}H NMR (400 MHz, $CDCl_3$) δ 8.76 (d, *J* = 1.3 Hz, 1H), 8.73-8.72 (dd, *J* = 2.5, 1.6 Hz, 1H), 8.57 (d, *J* = 2.5 Hz, 1H), 7.47-.44 (m, 1H), 7.40-7.32 (m, 3H), 2.43 (s, 3H); ^{13}C NMR (100 MHz, $CDCl_3$) δ 155.8, 144.7, 143.9, 142.0, 136.4, 136.3, 131.1, 129.8, 129.4, 126.2, 20.3.

2,6-diphenylpyrazine (19x)

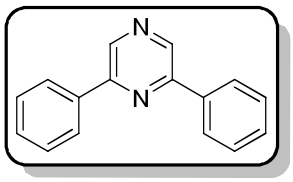

White solid; ^{1}H NMR (400 MHz, $CDCl_3$) δ 9.00 (s, 2H), 8.19 (d, *J* = 6.8 Hz, 4H), 7.62-7.50 (m, 6H); ^{13}C NMR (100 MHz, $CDCl_3$) δ 152.6, 137.7, 135.9, 130.4, 129.1, 127.1.

2,6-di(naphthalen-1-yl)pyrazine (19y)

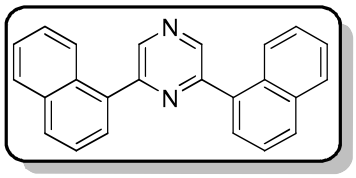

White solid; ^{1}H NMR (400 MHz, $CDCl_3$) δ 8.98 (s, 2H), 8.32-8.22 (m, 2H), 8.05-7.95 (m, 4H), 7.81 (d, *J* = 6.7 Hz, 2H), 7.65 (t, *J* = 7.4 Hz, 2H), 7.58 (dd, *J* = 6.1, 2.9 Hz, 4H); ^{13}C NMR (100 MHz, $CDCl_3$) δ 154.5, 143.3, 133.9, 133.1, 130.8, 130.5, 128.7, 128.6, 127.3, 126.4, 125.3, 124.6.

4.4 Conclusions

In the present work, synthesis and characterization of imidazolium-based quinoline ligand **L2H** and its abnormal NHC/CNN pincer palladium(II) complex **L2PdBr** are discussed. The NMR studies and crystallography data suggested the abnormal binding of palladium *via* C5 carbon atom of the imidazolium ring. Also, complex **L2PdBr** showed good catalytic activity for the Suzuki-Miyaura cross-coupling of aryl chlorides with arylboronic acids. The reaction was completed under microwave irradiation utilizing mild base and water as a solvent. Simple synthetic route for air and moisture stable catalyst, the good catalytic application under

aqueous condition, and utilization of aryl chlorides as substrates are the few advantages of the present study.

4.5 References

[1] Yu, D.; Bai, J.; Wang, J.; Liang, H.; Li, C. *Applied Surface Science* **2017**, *399*, 185-191.

[2] Korzec, M.; Bartczak, P.; Niemczyk, A.; Szade, J.; Kapkowski, M.; Zenderowska, P.; Balin, K.; Lelątko, J.; Polanski, J. *Journal of Catalysis* **2014**, *313*, 1-8.

[3] Campo, M. A.; Zhang, H.; Yao, T.; Ibdah, A.; McCulla, R. D.; Huang, Q.; Zhao, J.; Jenks, W. S.; Larock, R. C. *Journal of the American Chemical Society* **2007**, *129*, 6298-6307.

[4] Trejos, A.; Fardost, A.; Yahiaoui, S.; Larhed, M. *Chemical Communications* **2009**, 7587-7589.

[5] Xia, Y.; Qiu, D.; Wang, J. *Chemical Reviews* **2017**, *117*, 13810-13889.

[6] Choi, J.; Fu, G. C. *Science* **2017**, *356*, 7230-7240.

[7] Heravi, M. M.; Heidari, B.; Ghavidel, M.; Ahmadi, T. *Current Organic Chemistry* **2017**, *21*, 2249-2313.

[8] Biffis, A.; Centomo, P.; Del Zotto, A.; Zecca, M. *Chemical Reviews* **2018**, *118*, 2249-2295.

[9] Beletskaya, I. P.; Alonso, F.; Tyurin, V. *Coordination Chemistry Reviews* **2019**, *385*, 137-173.

[10] Hooshmand, S. E.; Heidari, B.; Sedghi, R.; Varma, R. S. *Green Chemistry* **2019**, *21*, 381-405.

[11] Kaur, N. *Catalysis Reviews* **2015**, *57*, 1-78.

[12] Liu, G.; Han, F.; Liu, C.; Wu, H.; Zeng, Y.; Zhu, R.; Yu, X.; Rao, S.; Huang, G.; Wang, J. *Organometallics* **2019**, *38*, 1459-1467.

[13] Littke, A. F.; Fu, G. C. *Angewandte Chemie International Edition* **2002**, *41*, 4176-4211.

[14] Nguyen, H. N.; Huang, X.; Buchwald, S. L. *Journal of the American Chemical Society* **2003**, *125*, 11818-11819.

[15] Kinzel, T.; Zhang, Y.; Buchwald, S. L. *Journal of the American Chemical Society* **2010**, *132*, 14073-14075.

[16] Yin, J.; Buchwald, S. L. *Journal of the American Chemical Society* **2000**, *122*, 12051-

12052.

[17] Cammidge, A. N.; Crepy, K. V. L. *Chemical Communications* **2000**, 1723-1724.

[18] Amatore, C.; Jutand, A.; Le Duc, G. *Chemistry – A European Journal* **2011**, *17*, 2492-2503.

[19] Biajoli, A. F. P.; Schwalm, C. S.; Limberger, J.; Claudino, T. S.; Monteiro, A. L. *Journal of the Brazilian Chemical Society* **2014**, *25*, 2186-2214.

[20] Boruah, P. R.; Ali, A. A.; Chetia, M.; Saikia, B.; Sarma, D. *Chemical Communications* **2015**, *51*, 11489-11492.

[21] Mondal, M.; Bora, U. *Green Chemistry* **2012**, *14*, 1873-1876.

[22] Boruah, P. R.; Ali, A. A.; Saikia, B.; Sarma, D. *Green Chemistry* **2015**, *17*, 1442-1445.

[23] Lu, F.; Ruiz, J.; Astruc, D. *Tetrahedron Letters* **2004**, *45*, 9443-9445.

[24] Alimardanov, A.; Schmieder-van de Vondervoort, L.; de Vries, A. H. M.; de Vries, J. G. *Advanced Synthesis & Catalysis* **2004**, *346*, 1812-1817.

[25] Phan, N. T. S.; Van Der Sluys, M.; Jones, C. W. *Advanced Synthesis & Catalysis* **2006**, *348*, 609-679.

[26] Goossen, L. J.; Koley, D.; Hermann, H. L.; Thiel, W. *Organometallics* **2006**, *25*, 54-67.

[27] Fairlamb, I. J. S.; Lee, A. F. *Organometallics* **2007**, *26*, 4087-4089.

[28] Huang, Y.-L.; Weng, C.-M.; Hong, F.-E. *Chemistry – A European Journal* **2008**, *14*, 4426-4434.

[29] Weng, C.-M.; Hong, F.-E. *Dalton Transactions* **2011**, *40*, 6458-6468.

[30] Wong, S. M.; Yuen, O. Y.; Choy, P. Y.; Kwong, F. Y. *Coordination Chemistry Reviews* **2015**, *293-294*, 158-186.

[31] Chow, W. K.; Yuen, O. Y.; So, C. M.; Wong, W. T.; Kwong, F. Y. *The Journal of Organic Chemistry* **2012**, *77*, 3543-3548.

[32] Wong, S. M.; So, C. M.; Chung, K. H.; Luk, C. H.; Lau, C. P.; Kwong, F. Y. *Tetrahedron Letters* **2012**, *53*, 3754-3757.

[33] Trzeciak, A. M.; Augustyniak, A. W. *Coordination Chemistry Reviews* **2019**, *384*, 1-20.

[34] Li, X.; Liu, C.; Wang, L.; Ye, Q.; Jin, Z. *ChemistrySelect* **2017**, *2*, 4016-4020.

[35] Hajipour, A.-R.; Rafiee, F. *Journal of the Iranian Chemical Society* **2015**, *12*, 1177-1181.

[36] Arumugam, V.; Kaminsky, W.; Bhuvanesh, N. S. P.; Nallasamy, D. *RSC Advances*

2015, *5*, 59428-59436.

[37] Sedighipoor, M.; Kianfar, A. H.; Mohammadnezhad, G.; Görls, H.; Plass, W. *Inorganica Chimica Acta* **2018**, *476*, 20-26.

[38] Boubakri, L.; Dridi, K.; Al-Ayed, A. S.; Özdemir, İ.; Yasar, S.; Hamdi, N. *Journal of Coordination Chemistry* **2019**, *72*, 516-527.

[39] GÜRBÜZ, N.; KARACA, E. Ö.; ÖZDEMİR, İ.; ÇETİNKAYA, B. *Turkish Journal of Chemistry* **2015**, *39*, 1115-1157.

[40] Majid, M. H.; Bahareh, H.; Mahdieh, G.; Tahereh, A. *Current Organic Chemistry* **2017**, *21*, 2249-2313.

[41] Xu, X.; Xu, B.; Li, Y.; Hong, S. H. *Organometallics* **2010**, *29*, 6343-6349.

[42] Vijaykumar, G.; Jose, A.; Vardhanapu, P. K.; P, S.; Mandal, S. K. *Organometallics* **2017**, *36*, 4753-4758.

[43] Kim, Y.; Lee, E. *Chemical Communications* **2016**, *52*, 10922-10925.

[44] Ghadwal, R. S.; Lamm, J.-H.; Rottschäfer, D.; Schürmann, C. J.; Demeshko, S. *Dalton Transactions* **2017**, *46*, 7664-7667.

[45] Yang, L.; Zhang, W.; Xiao, Y.; Mao, P. *ChemistrySelect* **2016**, *1*, 680-684.

[46] Chen, M.-T.; Kao, Z.-L. *Dalton Transactions* **2017**, *46*, 16394-16398.

[47] Steeples, E.; Kelling, A.; Schilde, U.; Esposito, D. *New Journal of Chemistry* **2016**, *40*, 4922-4930.

[48] Wang, T.; Xie, H.; Liu, L.; Zhao, W.-X. *Journal of Organometallic Chemistry* **2016**, *804*, 73-79.

[49] Seva, L.; Hwang, W.-S.; Sabiah, S. *Journal of Molecular Catalysis A: Chemical* **2016**, *418-419*, 125-131.

[50] Garrido, R.; Hernández-Montes, P. S.; Gordillo, Á.; Gómez-Sal, P.; López-Mardomingo, C.; de Jesús, E. *Organometallics* **2015**, *34*, 1855-1863.

[51] Sau, S. C.; Santra, S.; Sen, T. K.; Mandal, S. K.; Koley, D. *Chemical Communications* **2012**, *48*, 555-557.

[52] Rottschäfer, D.; Schürmann, C. J.; Lamm, J.-H.; Paesch, A. N.; Neumann, B.; Ghadwal, R. S. *Organometallics* **2016**, *35*, 3421-3429.

[53] Taakili, R.; Lepetit, C.; Duhayon, C.; Valyaev, D. A.; Lugan, N.; Canac, Y. *Dalton Transactions* **2019**, *48*, 1709-1721.

[54] Zuo, W.; Braunstein, P. *Dalton Transactions* **2012**, *41*, 636-643.

[55] Andrew, R. E.; González-Sebastián, L.; Chaplin, A. B. *Dalton Transactions* **2016**, *45*,

1299-1305.

[56] Wei, W.; Qin, Y.; Luo, M.; Xia, P.; Wong, M. S. *Organometallics* **2008**, *27*, 2268-2272.

[57] Inés, B.; SanMartin, R.; Moure, M. J.; Domínguez, E. *Advanced Synthesis & Catalysis* **2009**, *351*, 2124-2132.

[58] Imanaka, Y.; Shiomoto, N.; Tamaki, M.; Maeda, Y.; Nakajima, H.; Nishioka, T. *Bulletin of the Chemical Society of Japan* **2016**, *90*, 59-67.

[59] Haque, R. A.; Asekunowo, P. O.; Budagumpi, S.; Shao, L. *European Journal of Inorganic Chemistry* **2015**, *2015*, 3169-3181.

[60] Jose, A.; Vijaykumar, G.; Vardhanapu, P. K.; Mandal, S. K. *Journal of Organometallic Chemistry* **2018**, *865*, 51-57.

[61] Lee, J.-Y.; Lee, J.-Y.; Chang, Y.-Y.; Hu, C.-H.; Wang, N. M.; Lee, H. M. *Organometallics* **2015**, *34*, 4359-4368.

[62] Shinde, V. N.; Bhuvanesh, N.; Kumar, A.; Joshi, H. *Organometallics* **2020**, *39*, 324-333.

[63] Liu, Y.; Hartman, R. L. *Reaction Chemistry & Engineering* **2019**, *4*, 1341-1346.